How the dilatancy of soils affects their behavior

Article · January 1991

CITATIONS
60

READS
3,440

1 author:

Guy Tinmouth Houlsby
University of Oxford
296 PUBLICATIONS **8,969** CITATIONS

SEE PROFILE

HOW THE DILATANCY OF SOILS AFFECTS THEIR BEHAVIOUR

by

G.T. Houlsby

The written version of an invited lecture delivered at the Tenth European Conference on Soil Mechanics and Foundation Engineering, Florence, Italy, 28th May 1991

Report Number OUEL 1888/91

Soil Mechanics Report Number 121/91

University of Oxford,
Department of Engineering Science,
Parks Road,
Oxford
OX1 3PJ
U.K

Tel. (0865) 283300
Fax. (0865) 283301

How the Dilatancy of Soils Affects Their Behaviour

De la Manière dont la Dilatance des Sols Influence Leur Comportement

G.T. Houlsby

Department of Engineering Science, Oxford University, U.K.

ABSTRACT: The relationships between the friction angle, dilation angle, density and pressure in a granular material are explored. The link between friction and dilation is well established, but quantitative expressions for the dependance of dilation on density and pressure are less well known. A new relationship based on the concepts of Critical State Soil Mechanics is suggested. The types of problem in which dilation plays an important rôle are then examined, and it is seen that dilatancy increases in significance for heavily constrained problems. The influence of dilation on the capacity of piles is treated in more detail. Additional topics treated include the generalisation of dilation expressions.

RÉSUMÉ: Les relations entre l'angle de frottement, l'angle de dilatance, la densité et la pression dans un milieu granulaire sont étudiées. Le lien entre frottement et dilatance est bien établi, mais les expressions quantitatives de l'influence de la densité et de la pression sur la dilatance sont moins bien connues. Une nouvelle relation basée sur les concepts de la Mécanique des Sols de l'État Critique est proposée. Les types de problèmes dans lesquels la dilatance joue un rôle important sont ensuite examinés, et il est montré que la dilatance croît d'une manière significative dans les problèmes à déformation empêchée. L'infuence de la dilatance sur la capacité portante des pieux est traitée d'une manière plus détaillée. Les aspects complémentaires qui sont traités incluent la généralisation des expressions de la dilatance.

1 PREAMBLE

Professor Peter Wroth, of Oxford University, was invited to present a lecture at the Tenth European Conference on Soil Mechanics and Foundation Engineering, and chose as his subject the title of this paper. Sadly, Professor Wroth died in February 1991, and the Author was invited to present a lecture on the same topic in his place. Professor Wroth had not written his lecture, and so this paper is the Author's own views on the subject. The lecture at the Conference, and this written version of it, are presented as the Author's personal tribute to Professor Wroth's wisdom as an engineer, and in gratitude for his many years of encouragement and support.

2 INTRODUCTION

This Paper is divided into two main parts. In the first the relationships between friction, dilation, density and pressure are explored. It is seen that the relationship between the friction angle and dilation angle is well established both theoretically and experimentally. Relationships between the dilation angle and density and pressure are equally important, although less well established quantitatively. Dilation will be seen as occupying a central role in explaining phenomena such as the reduction of angle of friction with increasing stress level.

In the second part of the Paper a series of problems are examined to establish the cases where dilation is important, and it is seen that dilation assumes increasing significance as problems become more kinematically constrained. Particular emphasis is placed in this section on the role of dilation in calculations of the capacity of piles.

Some additional topics are treated at the end of the paper.

3 FRICTION, DILATION, DENSITY AND PRESSURE

The simple frictional model for the failure of a soil, based on Coulomb's pioneering work in 1773, is familiar to all geotechnical engineers, and is conveniently shown on the Mohr's circle diagram, Figure 1. The frictional relationship must of course be expressed in terms of effective, not total, stresses. In the remainder of this Paper the term *stress* shall always mean *effective stress*, and will be indicated by a prime (′). The friction angle ϕ' is used to describe the strength of the soil.

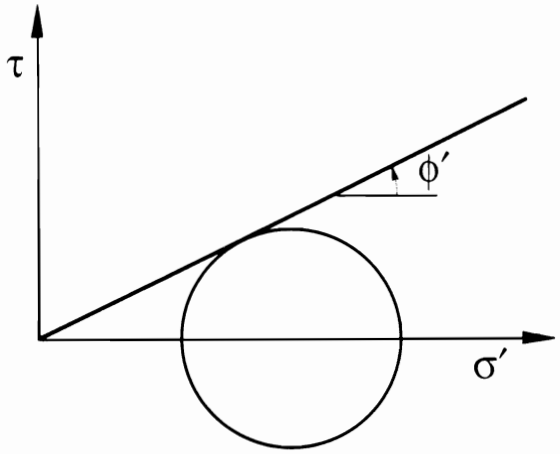

Figure 1, The Mohr-Coulomb failure criterion

Closer examination reveals that the behaviour of soils is more subtle, and shows a number of important features. Firstly, in a test such as the simple shear test on a dense sand, a peak is usually observed in the shear stress - shear strain relationship, followed by a reduction in shear stress at large strain, Figure 2. Similar peaks are observed in other types of shear test. A careful distinction between the peak and large strain angles of friction is therefore necessary, and they are called here ϕ'_p and ϕ'_{cv}.

If the vertical movements, as well as shear displacements, are measured in a simple shear test, then a dense sand usually dilates, that is it expands in volume, as the test proceeds. The dilation usually takes place after a small initial compression, Figure 3. The magnitude of the dilation depends very strongly on the density of the soil, with denser samples expanding more rapidly.

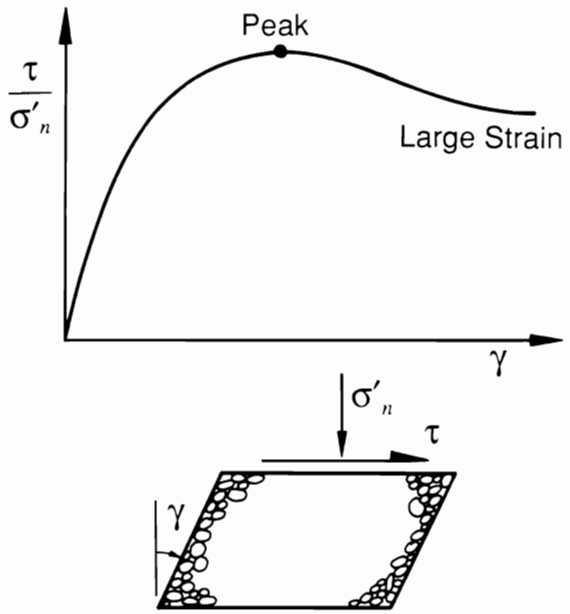

Figure 2, Typical shear stress - shear strain curve in simple shear test

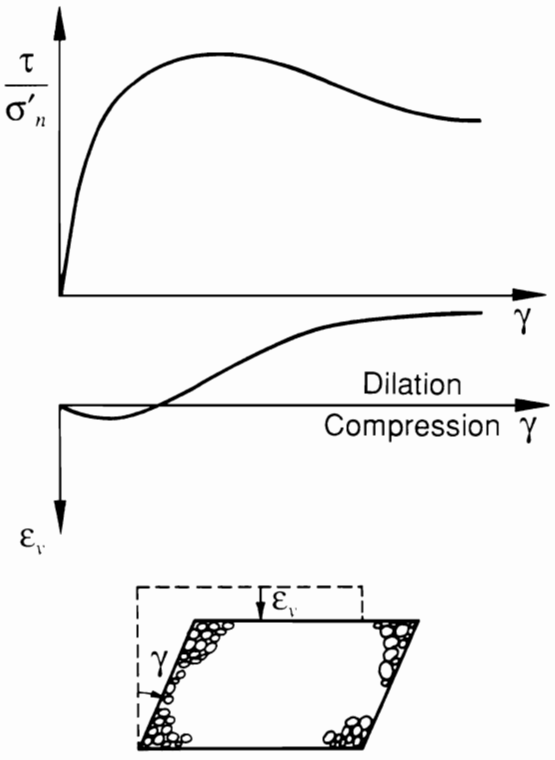

Figure 3, Dilation of dense sand in a simple shear test

If tests are carried out at a number of normal stress levels, it is found that the peak angle of friction reduces with increasing stress level. The result is that the peak strength envelope is curved in the Mohr-Coulomb plot, Figure 4. The peak friction angle approaches the large strain friction angle at very high stress levels.

The features of (a) peak and large strain angles of friction, (b) dilation and the (c) reduction of peak strength with stress level appear at first to be disconnected, and perhaps confusing, phenomena. An important step in the understanding of soil behaviour is the realisation that these features are in fact closely connected, and the understanding of the rôle of dilation is the key to the understanding of how these phenomena are linked. The first step is to appreciate the link between the angles of

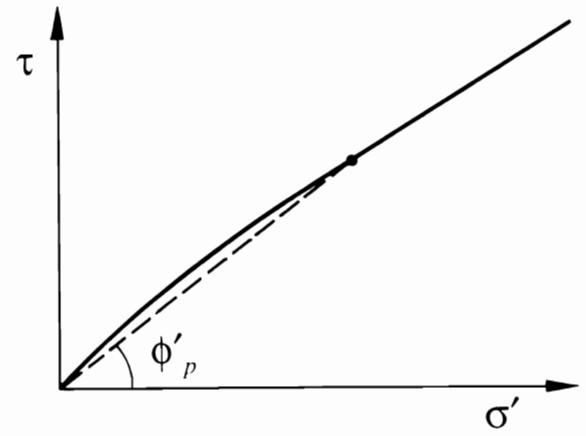

Figure 4, Curved peak strength envelope on Mohr's circle plot

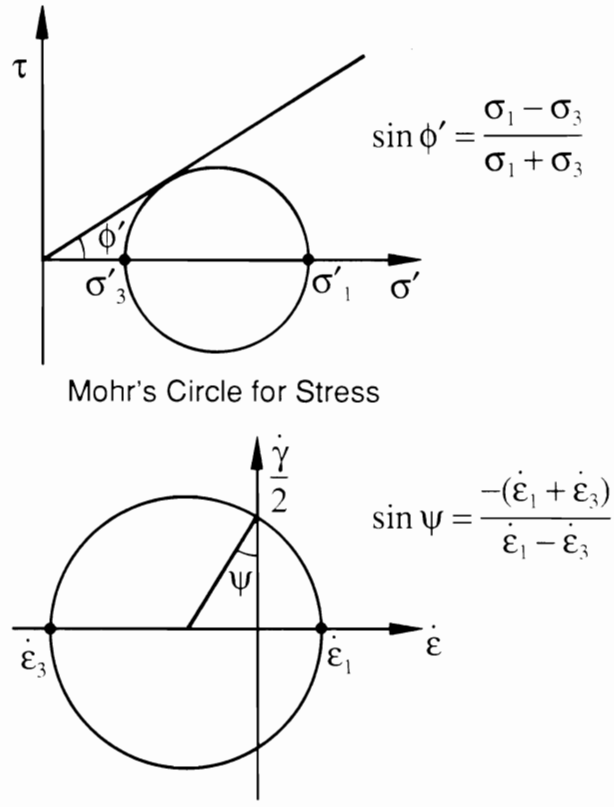

Figure 5, Definitions of the angles of friction and dilation

friction and of dilation; it is then possible to relate the angle of dilation to the density and pressure.

The quantities we must first define are as follows. The angle of friction ϕ' expresses the ratio of a shear stress to a normal stress, and can be defined in terms of principal stresses, Figure 5:

$$\sin\phi' = \frac{\sigma'_1 - \sigma'_3}{\sigma'_1 + \sigma'_3} \qquad \ldots(1)$$

In a similar way the angle of dilation ψ (the symbol ν is also sometimes used for dilation angle) expresses the ratio between a volumetric strain rate and a shear strain rate. For the case of plane strain ($\varepsilon_2 = 0$) it can be defined in terms of the principal strain rates (Figure 5):

$$\sin\psi = \frac{-(\dot{\varepsilon}_1 + \dot{\varepsilon}_3)}{\dot{\varepsilon}_1 - \dot{\varepsilon}_3} \qquad \ldots(2)$$

The minus sign in Equation 2 arises simply from the convention that compressive stresses and strains are taken as positive in soil mechanics, and is introduced so that the angle of dilation is positive when the soil expands.

The superposed dots used in Equation 2 to indicate the strain rates do not imply that the process is in any way dynamic. The term *rate* is being used here in the sense used in plasticity theory, in which the time increment is artificial. The equation could just as well be expressed in terms of strain increments $\delta\varepsilon$ rather than strain rates $\dot{\varepsilon}$.

It is important to note that whilst the definition of the angle of friction remains unchanged for different stress conditions (e.g. triaxial compression, plane strain, triaxial extension), the extension of the definition of the angle of dilation to other than plane strain conditions needs to be treated with more care. The usual definition employed is:

$$\sin\psi = \frac{-(\dot{\varepsilon}_1 + \dot{\varepsilon}_2 + \dot{\varepsilon}_3)}{\dot{\varepsilon}_1 - \dot{\varepsilon}_3} \qquad \ldots(3)$$

which reduces to Equation 2 for plane strain conditions.

A more important distinction is that the angle of dilation should strictly be defined in terms of the *plastic components* of the strain rates, not the total strain rates. If the strain ε is divided into elastic (recoverable) and plastic (irrecoverable) components:

$$\varepsilon = \varepsilon^e + \varepsilon^p \qquad \ldots(4)$$

then Equation 2 should be modified to:

$$\sin\psi = \frac{-(\dot{\varepsilon}_1^p + \dot{\varepsilon}_3^p)}{\dot{\varepsilon}_1^p - \dot{\varepsilon}_3^p} \qquad \ldots(5)$$

In theory this important distinction means that the determination of the angle of dilation from a test becomes much more difficult, since it depends on the estimate which is made for the elastic properties of the soil. In practice the distinction is less important since (for most soils, under most test conditions) the elastic stiffness is sufficiently high that the elastic strains are much smaller than the plastic strains and the difference between Equations 2 and 5 is small. In particular, at the peak in several commonly used shear tests the stresses are not changing, so the elastic strain rates are zero and Equations 2 and 4 coincide. In the remainder of this paper it will be assumed that the elastic strain rates are sufficiently small that Equation 2 can be used with adequate accuracy.

The simplest way to understand the relationship between the angles of friction and dilation is to make use of a physical analogy: the sawtooth model, see Figure 6.

If one frictional block slides over another on a flat plane, with an angle of friction on the plane ϕ'_{cv} (i.e. a coefficient of friction $\mu = \tan\phi'_{cv}$) Then the ratio of the shear to the normal stress is:

$$\frac{\tau}{\sigma'_n} = \tan\phi'_{cv} \qquad \ldots(6)$$

The choice of the subscript "cv" is to indicate that in this case the shearing takes place at constant volume, i.e. no dilation occurs.

If we consider sliding on a rough plane, represented by a sawtooth with teeth at an angle ψ to the horizontal, with the same angle of friction ϕ'_{cv} as above acting on the teeth of the saw, then simple statics can be used to derive the relationship between the observed shear and normal stress when sliding occurs. This ratio could be termed $\tan\phi'$, where ϕ' is the observed angle of friction. It can easily be shown that:

$$\frac{\tau}{\sigma'_n} = \tan\phi' = \tan(\phi'_{cv} + \psi) \qquad \ldots(7)$$

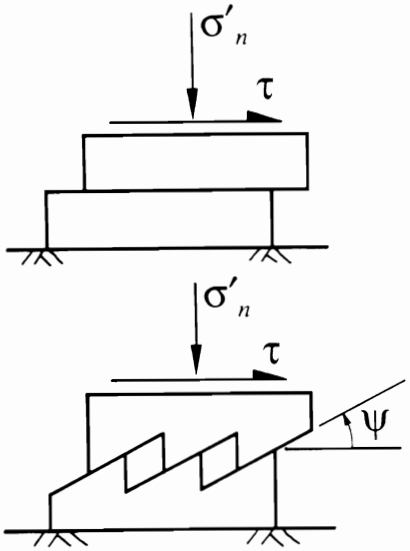

Figure 6, The sawtooth model for dilatancy

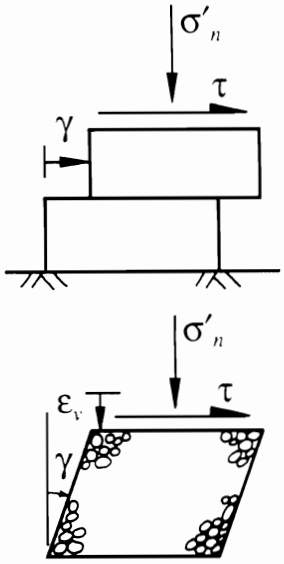

Figure 7, Analogy used in Taylor's energy correction

so that $\phi' = \phi'_{cv} + \psi$, and the observed angle of friction is the sum of the angle of friction at constant volume and the angle of dilation. This type of relationship is called a flow rule.

A variety of other more sophisticated theories have been put forward to explain the relationship between the friction and dilation angles, some of which are discussed below.

One of the first approaches to explain the connection was made by Taylor (1948) who suggested an "energy correction" to account for dilation. In more modern terminology Taylor's expression can be viewed as a hypothesis about the dissipation of work in a frictional soil. All frictional relationships can be viewed in terms of dissipation of energy rather than directly in terms of forces. For a block sliding on a smooth plane (Figure 7), the rate of input work is:

$$\dot{W} = \tau\dot{\gamma} \qquad \ldots(8)$$

and if we adopt the hypothesis that this work is dissipated internally in a way which is proportional to the normal stress σ'_n and the shear strain rate $\dot{\gamma}$, then we have:

$$\dot{W} = (\tan\phi'_{cv})\sigma'_n\dot{\gamma} \qquad \ldots(9)$$

where the constant of proportionality is $\tan\phi'_{cv}$. Combining Equations (8) and (9) yields the familiar result $\tau/\sigma'_n = \tan\phi'_{cv}$.

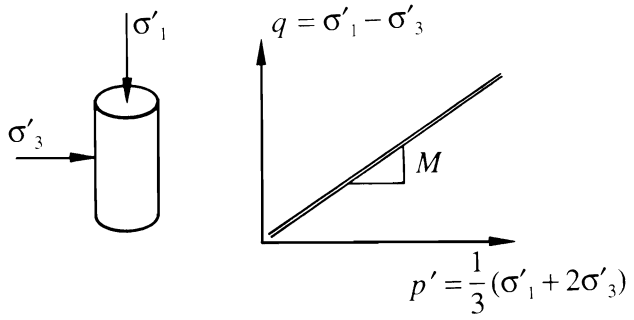

Figure 8, Triaxial parameters used for definition of the Cam-Clay flow rule

The same hypothesis is adopted for a sample of soil in simple shear: that the dissipated work is proportional to the normal stress and the shear strain rate. This time, however, the input work includes a term in σ'_n multiplied by $\dot{\varepsilon}_v$, since dilation may take place and so the normal stress as well as the shear stress does work. The result is therefore:

$$\dot{W} = \sigma'_n \dot{\varepsilon}_v + \tau\dot{\gamma} = (\tan\phi'_{cv})\sigma'_n\dot{\gamma} \qquad ...(10)$$

Noting that we could define the apparent angle of friction by $\tan\phi' = \tau/\sigma'_n$, and that the angle of dilation is given by $\tan\psi = -\dot{\varepsilon}_v/\dot{\gamma}$, then Equation 10 can be rearranged to give:

$$\tan\phi' = \tan\phi'_{cv} + \tan\psi \qquad ...(11)$$

which differs slightly from the result from the sawtooth model, but again expresses the notion that the angle of friction is equal to the sum of the angle of friction at constant volume and a term which depends on the rate of dilation.

Very similar concepts were used in the development of the Cam-Clay model for soil behaviour (Schofield and Wroth, 1968). The results are usually expressed in terms appropriate for the triaxial test, see Figure 8, and use the stress and strain invariants:

$$p' = \frac{1}{3}(\sigma'_1 + 2\sigma'_3) \qquad ...(12)$$

$$q = \sigma'_1 - \sigma_3 \qquad ...(13)$$

$$v = \varepsilon_1 + 2\varepsilon_3 \qquad ...(14)$$

$$\varepsilon = \frac{2}{3}(\varepsilon_1 - \varepsilon_3) \qquad ...(15)$$

The Cam-Clay work hypothesis is expressed as:

$$\dot{W} = p'\dot{v} + q\dot{\varepsilon} = Mp'\dot{\varepsilon} \qquad ...(16)$$

which can be seen to be a direct analogy of Taylor's expression (Equation 10). On rearrangement it gives:

$$\frac{q}{p'} = M - \frac{\dot{v}}{\dot{\gamma}} \qquad ...(17)$$

which again gives a measure of the angle of friction (q/p', actually equal to $6\sin\phi'/(3-\sin\phi')$), equal to a constant (M) plus a measure of the angle of dilation ($-\dot{v}/\dot{\varepsilon}$, actually equal to $(3\sin\psi)/2$).

The approach taken by Rowe (1962) in the development of his stress-dilatancy theory is conceptually quite different, although it leads to a very similar result. Rowe examined first the properties regular assemblies of spheres, and was able to obtain expressions for both the stress ratio σ'_1/σ'_3 and the strain rate ratio $-\dot{\varepsilon}_3/\dot{\varepsilon}_1$ in terms of the geometry of packing. He then assumed that analogies could be drawn with irregular packings of soil particles. He assumes that sliding takes place on a

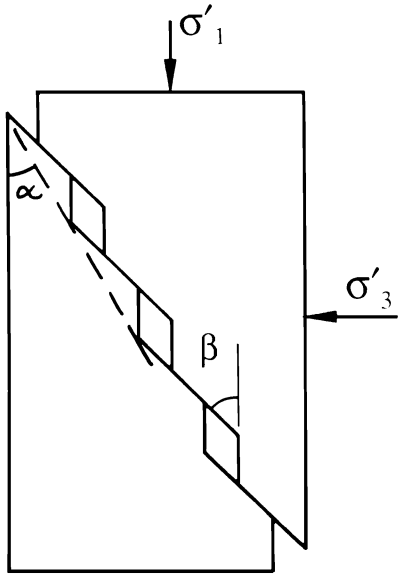

Figure 9, Assumed sliding mechanism for Rowe's stress-dilatancy flow rule

sawtoothed plane, see Figure 9, and these ratios are therefore functions of the angles α and β. The functions are such that α can be eliminated to give:

$$\frac{\sigma'_1}{\sigma'_3} = \frac{\tan(\phi_\mu + \beta)}{\tan\beta}\frac{-\dot{\varepsilon}_3}{\dot{\varepsilon}_1} \qquad ...(18)$$

where ϕ_μ is the fundamental angle of friction for grain-to-grain contact. Rowe then adopts a minimum energy *ratio* hypothesis to derive $\beta = \pi/4 - \phi_\mu/2$, but the same result can also be obtained by assuming a minimum stress ratio at a given strain rate ratio. The final result is:

$$\frac{\sigma'_1}{\sigma'_3} = \tan^2\left(\frac{\pi}{4} + \frac{\phi_\mu}{2}\right)\left(\frac{-\dot{\varepsilon}_3}{\dot{\varepsilon}_1}\right) \qquad ...(19)$$

which is often written in the short form $R = KD$. The precise rôle of ϕ_μ now becomes unclear, since it now appears as the angle of friction at constant volume. Experimental evidence is, however, that this is not equal to the grain-to-grain friction angle. The discrepancy has been a matter of some debate.

All the methods described above establish theoretical reasons for a connection between the angles of friction and dilation. Experimental evidence for the theories has been presented both by the originators of the theories and by other researchers. Alternatively one could take a mainly empirical approach. Bolton (1986) presented a particularly comprehensive review of the experimental data on friction and dilation angles, and suggested a very simple empirical fit to the data:

$$\phi'_p = \phi'_{cv} + 0.8\psi_{max} \qquad ...(20)$$

If the various methods (for the plane strain case) are compared, it can be seen from Figure 10, that the differences are relatively small. Of the theoretical expressions Rowe's falls in the middle of the range, and Bolton's empirical expression matches Rowe's very closely.

It should be noted that these flow rules can be applied in two distinct senses. Firstly they may be used to express the relationship between the *mobilised* angle of friction and the *current* dilation rate as a test progresses. Secondly they may be used to express the relationship between the *peak* friction angle and the *maximum* dilation rate for several tests on the same material. Bolton's empirical relationship is based on the observations of the latter type.

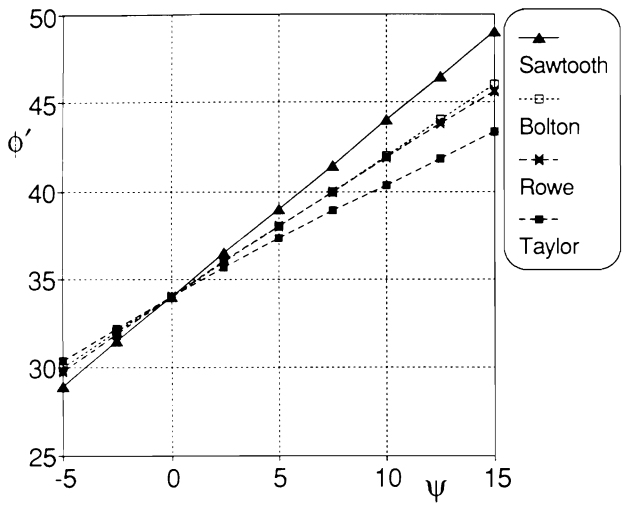

Figure 10, Comparison of flow rules

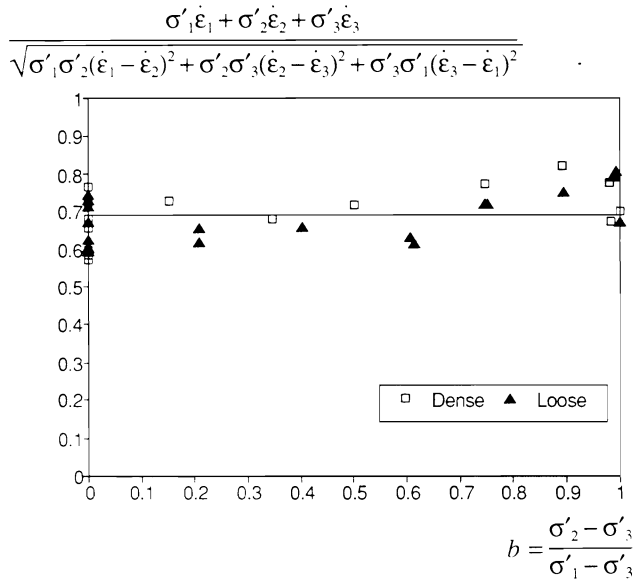

Figure 11, Variation with measured ϕ'_{cvtc} with mode of shearing

One problem in the use of the above flow rules is that the constants employed in them (i.e. ϕ'_{cv}, M or ϕ_μ) need to be changed for different modes of shearing, as the angle of friction at constant volume in plane strain is typically a few degrees higher than that in triaxial compression. Bolton specifically assumes the two angles to be equal, but this is not supported by the experimental evidence. The Author has found that the following work hypothesis provides a flow rule which fits the data from tests with different modes of shearing well:

$$\dot{W} = \sigma'_1\dot{\varepsilon}_1 + \sigma'_2\dot{\varepsilon}_2 + \sigma'_3\dot{\varepsilon}_3 =$$

$$\frac{\sqrt{8}}{3}\tan\phi'_{cvtc}\sqrt{\sigma'_1\sigma'_2(\dot{\varepsilon}_1-\dot{\varepsilon}_2)^2+\sigma'_2\sigma'_3(\dot{\varepsilon}_2-\dot{\varepsilon}_3)^2+\sigma'_3\sigma'_1(\dot{\varepsilon}_3-\dot{\varepsilon}_1)^2} \quad \ldots(21)$$

where ϕ'_{cvtc} is the angle of friction at constant volume in triaxial compression. Figure 11 shows the implied values of ϕ'_{cvtc} evaluated from the peak points from true triaxial tests on sand (Lade, 1972), and shows that this parameter is almost independent of the mode of shearing.

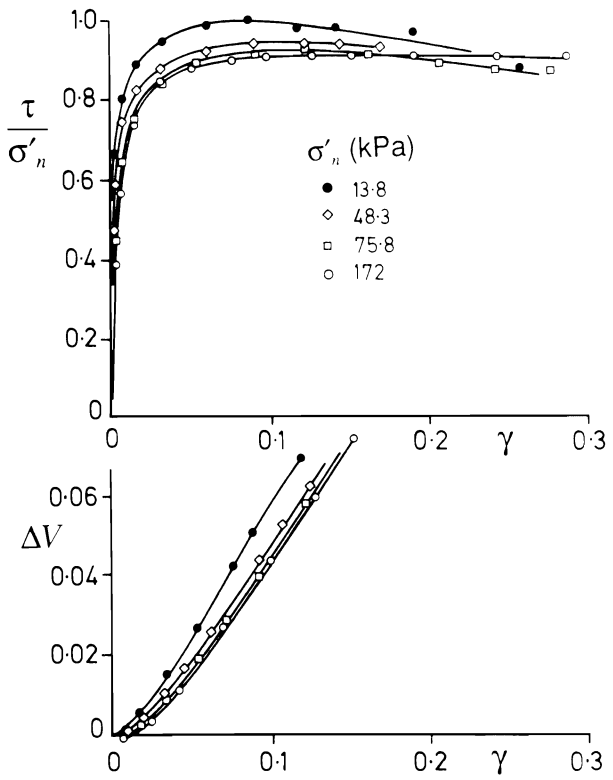

Figure 12, Shear stress - shear strain and volumetric strain - shear strain for simple shear tests on sand (after Stroud, 1971)

It is clear from the above discussion that the relationship between friction and dilation is firmly established both theoretically and experimentally. Although the details of the approaches taken by various authors may differ, the broad conclusions are the same. We turn now to the relationship between dilation and density. It is expected that the denser a sand is the more it will tend to expand, i.e. the higher the dilation angle will be. We find that although this trend is well known, quantitative expressions for the variation of dilation rate with density are much less well established.

One of the best ways of examining the stress-strain behaviour of soils is by simple shear tests, and Stroud (1974) carried out a particularly well controlled set of these tests at Cambridge. The term "simple" refers to the mode of shearing applied to the sample: the apparatus used for the test is in fact rather complex. The upper graph in Figure 12 shows the shear stress-strain curves for his tests on dense sand and the lower curves the change in specific volume with shear strain. Each of these tests started at about the same density, and all showed about the same angle of dilation.

Wroth (1958) had earlier carried out simple shear tests on a variety of materials. These experiments were some of those which formed the basis of what later became known as Critical State Soil Mechanics. Figure 13 shows a set of tests on steel balls, initially packed at different densities. The rate of dilation is higher for denser samples, i.e. those initially at a lower voids ratio. The samples dilate until they reach the same critical voids ratio, irrespective of their initial density, at which they can continue to shear with no further changes of density. The concept of critical voids ratio was not new, being due to Casagrande (1936).

The critical voids ratio is, however, not unique, since it reduces slightly with increasing normal stress. In Figure 14 the end points (i.e. the points where no further changes in voids ratio are occurring) of all of Stroud's tests on sand are plotted in the form of specific volume against mean stress. The points clearly fall on a single line in this plot, with the critical voids ratio reducing with pressure. This leads to the concept of the critical state line. On shearing, all samples will approach this

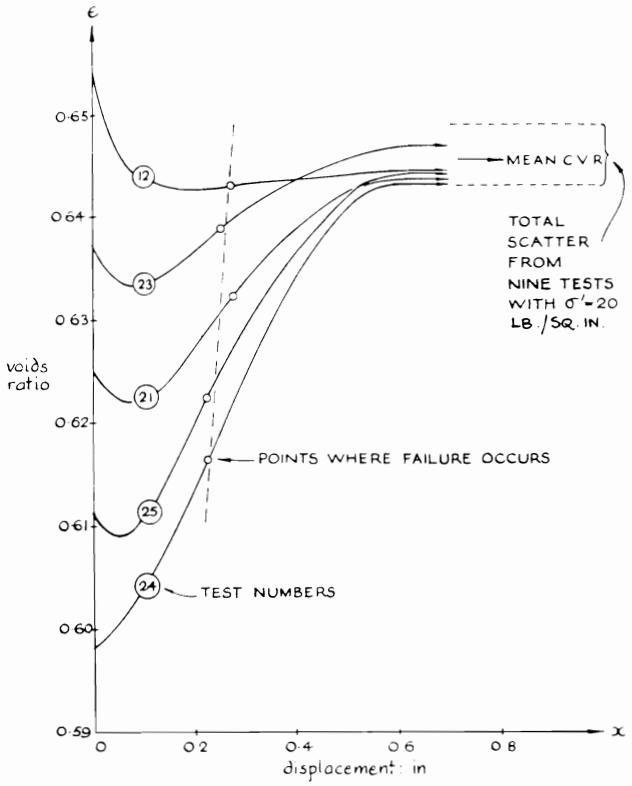

Figure 13, Voids ratio against shear displacement for simple shear tests on steel balls (from Wroth, 1958)

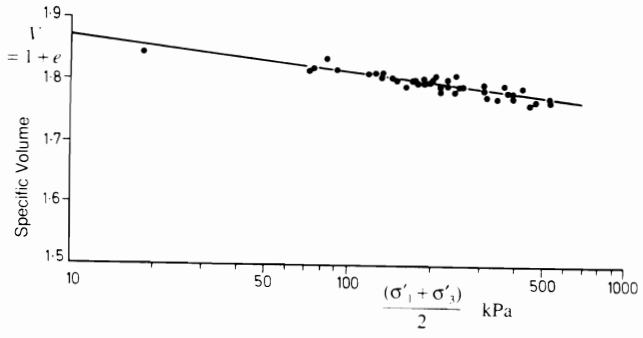

Figure 14, Critical State Line for simple shear tests on sand (after Stroud, 1971)

line, and as they do so will shear with no further change of specific volume, but the actual specific volume they attain will be lower for samples subjected to higher normal pressures. It is observed empirically for clays that the critical state line is parallel to the normal compression line in the consolidation plot.

Stroud's tests covered a range of initial stresses and densities, and the peak angle of friction he observed is shown plotted against pressure in Figure 15. The primary controlling factor for the peak strength is seen to be the density, with denser samples giving a higher strength, but at a given density the angle of friction reduces slightly with increasing stress level. The reduction of the peak strength with stress level is linked to the slope of the critical state line, but in order to establish this connection it is necessary to define some additional quantities.

On the critical state line the rate of dilation is zero, and it seems reasonable that the rate of dilation should simply be a function of the distance of the current stress point from the critical state line. This is expressed by defining the quantities shown in Figure 16. The slope of the critical state line in the V:lnp' plot is λ, and its position is fixed by the value Γ of the

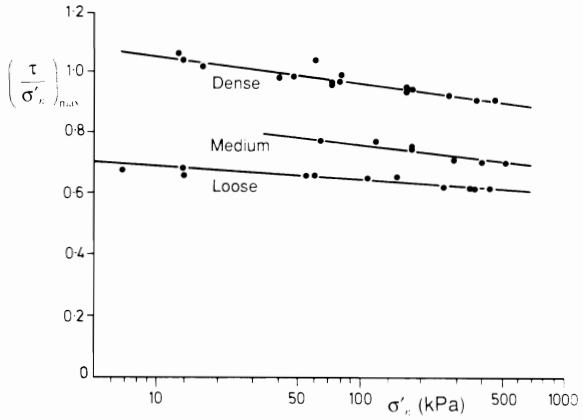

Figure 15, Peak strength against stress level for simple shear tests at different densities (after Stroud, 1971)

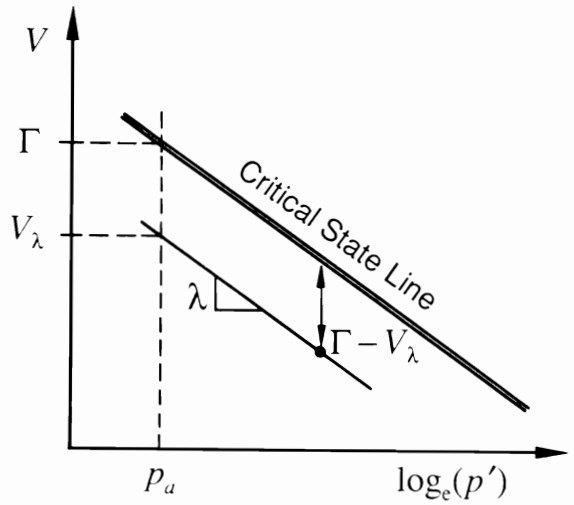

Figure 16, Definitions of Γ and V_λ

specific volume at some reference pressure p_a (conveniently taken as atmospheric pressure). The quantity V_λ, defined as $V + \lambda \ln(p'/p_a)$, is the value of V at p_a on a line drawn through the current point and parallel to the critical state line. Clearly the quantity $(\Gamma - V_\lambda)$ is the distance of the current point below the critical state line. This concept was originally suggested by Wroth and Bassett (1965), and has recently been rediscovered by Been and Jefferies (1985) in their use of the so-called "state parameter".

In Figure 17 the peak strengths from Stroud's tests are plotted against V_λ, and all the tests, from a variety of combinations of pressure and density, plot on a single curve. The peak strength is therefore a unique function of V_λ. In view of the relationships between friction and dilation angles already examined, this also means that the maximum dilation rate is a unique function of V_λ. It is perhaps most helpful to consider the latter relationship as the more fundamental: there are obvious physical reasons why the dilation rate should be higher for denser samples. This result establishes, at least qualitatively, the dependence of the friction and dilation angles on the pressure and density.

Wroth (private communication, 1990) replotted Stroud's data and suggested the simple expression $\sin\psi = \alpha(\Gamma - V_\lambda)$ for the variation of the angle of dilation with distance from the critical state line. The data are shown on Figure 18. The new quantity α is taken as a constant for any given sand, and Wroth found that values of α were typically near unity.

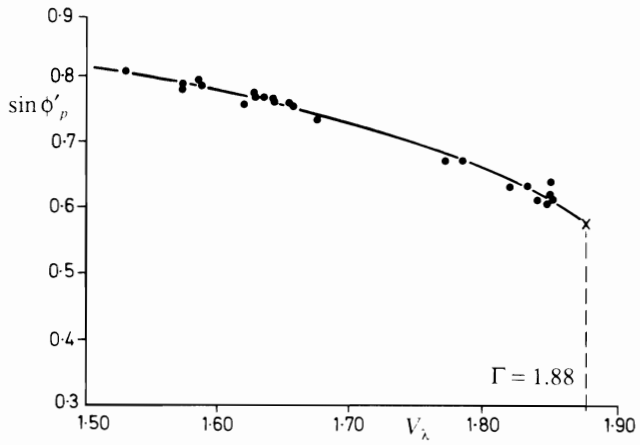

Figure 17, Peak strength plotted against V_λ (after Stroud, 1971)

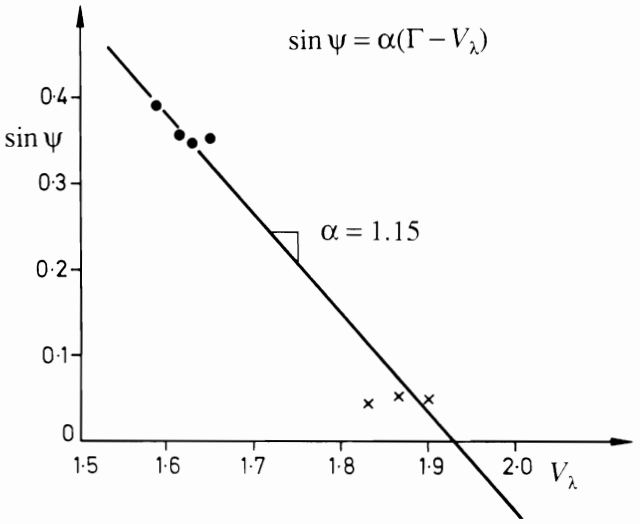

Figure 18, Wroth's interpretation of Stroud's simple shear tests on sand

In practice it is often more convenient to express the behaviour of sand as a function of the relative density I_D rather than the specific volume, and Wroth's expression can be reworked in these terms. The result is the expression:

$$\sin\psi = \alpha(\Gamma - V_{max}) + \alpha(V_{max} - V_{min})I_D - \alpha\lambda\ln\left(\frac{p'}{p_a}\right) \quad \ldots(22)$$

Although this expression looks complex, it is simply of the structure:

$$\sin\psi = A + BI_D - C\ln\left(\frac{p'}{p_a}\right) \quad \ldots(23)$$

where A, B and C are all simple functions of well defined properties of the soil. The angle of dilation (and therefore the angle of friction) increases with density and reduces with pressure. Equation 22 may be compared with the empirical expression suggested by Bolton (1986) for the angle of friction in plane strain (in degrees):

$$\phi'_p = \phi'_{cv} + 5\left(I_D\left[10 - \ln\left(\frac{p'}{1.5p_a}\right)\right] - 1\right) \quad \ldots(24)$$

Together with Equation 20, this can be used to derive an expression for the angle of dilation (in radians):

$$\psi = -0.11 + 0.59I_D - 0.11I_D\ln\left(\frac{p'}{p_a}\right) \quad \ldots(25)$$

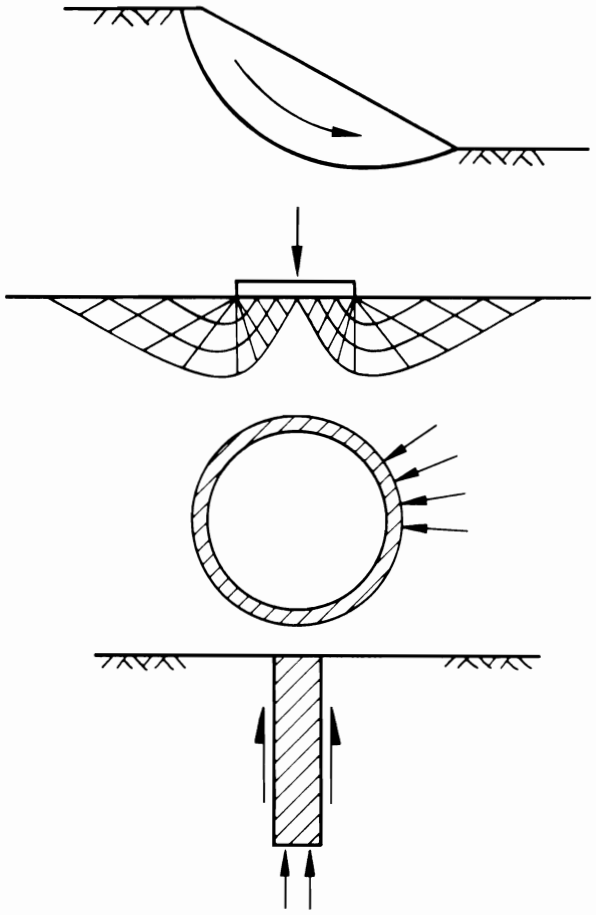

Figure 19, Example problems in increasing order of confinement

Equations 22 and 25 can be seen to be similar in structure, except for the last term. For the range of data available they give almost identical results, and Wroth's expression fits the data as well as Bolton's. Both express the concept that dilation rate (and hence strength) is primarily controlled by density, but also reduces with increasing stress level. The Author prefers Wroth's approach since (a) it directly embodies the concept of the critical state and (b) the constants required can be related to well defined measurable quantities.

If it is possible to estimate the density of a granular material, and the probable value of the working stresses, it is therefore possible to estimate first the dilation rate and then the peak angle of friction.

4 PROBLEMS IN WHICH DILATION IS IMPORTANT

We now examine some cases where the dilation of the soil is important. We should first note that dilation will always be important in that it will control the appropriate angle of friction. The purpose of this discussion is to examine cases where, in addition to this effect, the very fact that the soil is dilating has a further influence on the results.

The importance of dilation will be considered by examining four types of problem in geotechnical engineering, shown schematically in Figure 19. The examples have been ordered in a way that they represent increasing confinement of the soil. In a slope the soil is free to move in a relatively unconfined way. A footing and a flexible tunnel lining impose increasing levels of constraint on the way the soil can deform, and finally the soil in the vicinity of a pile is highly constrained. Intuitively we would expect that the more kinematically constrained the soil is, the more important dilation will be.

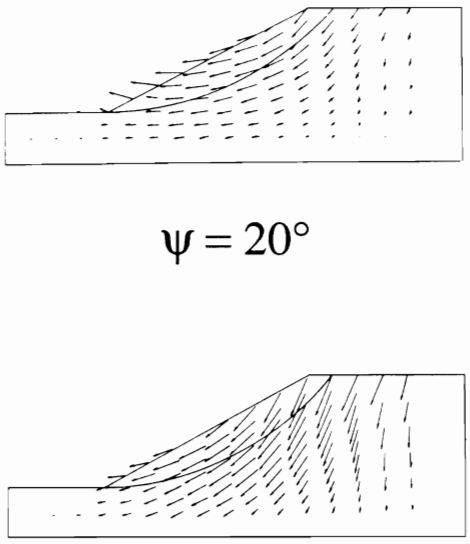

Figure 20, Deformations of a slope (after Zienciewicz, Humpheson and Lewis, 1975)

The influence of dilation on each of these problems must be examined theoretically, because only in theoretical or numerical analysis can the dilation rate be varied without simultaneously affecting other properties of the soil. Laboratory or field tests would be unable to distinguish the effects of dilation and of friction, since the two, as shown above, are linked for any given material.

The problem of slope stability was examined numerically by Zienciewicz, Humpheson and Lewis (1975). They used the finite element method to carry out two slope stability analyses in which they used the same angle of friction of 20°. In one they assumed the angle of dilation to be equal to the angle of friction, and in the other they assumed zero dilation. The first case in fact gives an impossibly high dilation rate. The analyses resulted in identical factors of safety. However, as would be expected, the patterns of deformation, shown in Figure 20, were rather different. Although this analysis involves a soil with a rather low friction angle, their conclusion that dilation in itself does not affect slope stability seems reasonable.

The problem of the bearing capacity of a footing was also examined by Zienciewicz *et al.* (1975), and they again observed no influence of the dilation rate. It was also examined by de Borst and Vermeer (1984), who carried out finite element analyses of both strip and circular footings on a material with an angle of friction of 40°. They used dilation angles of 40° and 20° (again the first value is impossibly high). The load-deformation curves for circular footings are shown in Figure 21, and the analysis with the higher angle of dilation shows a peak bearing capacity about 13% higher than for the lower dilation angle. At large deformations both analyses approach a similar capacity. It may be that the peak is an artefact of the particular numerical technique involved, but it is more likely that, at least for fairly high friction angles, the rate of dilation does have a small influence on the bearing capacity of a foundation.

As would be expected, the patterns of deformation around the footing, shown much exaggerated in Figure 22, are very different in the two cases. Much larger surface movements are observed for the larger angle of dilation.

The example of the tunnel was also studied by Zienciewicz *et al.* (1975), who made calculations for both the pressures on a tunnel lining, and the ground movements around it for various stages in the construction procedure. The details of the results

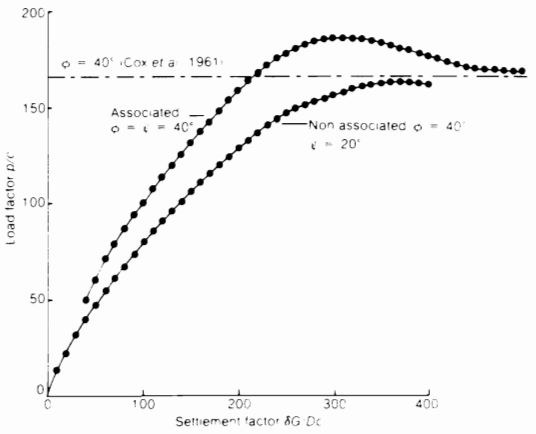

Figure 21, Load - deflection curves for circular footings (after de Borst and Vermeer, 1984)

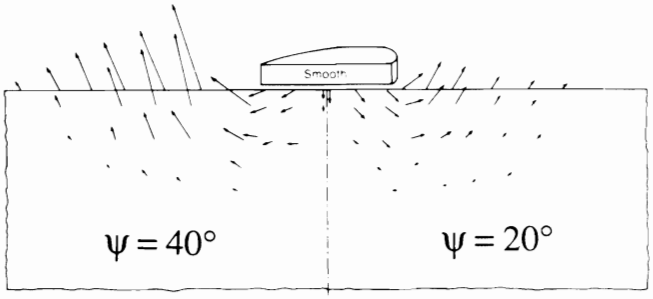

Figure 22, Deformations below a circular footing (after de Borst and Vermeer, 1984)

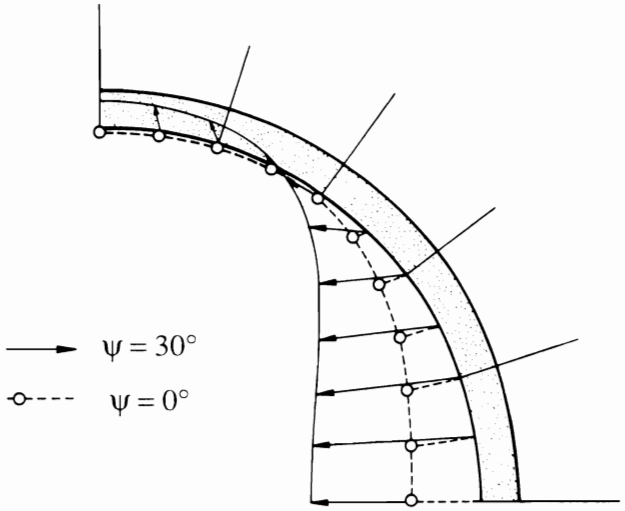

Figure 23, Deformations of a tunnel lining (after Zienciewicz, Humpheson and Lewis, 1975)

must be regarded as specific only to the case they examined, but an example of the influence of the dilation rate on the final deformation of the tunnel lining is shown in Figure 23. Much larger movements are observed for the more dilatant soil.

The conditions around a pile impose much more kinematic constraint on soil movements than for any of the previous problems. We would expect therefore that in a more dilatant soil higher stresses would develop. We shall examine now in rather more detail the influence of dilatancy on both the end bearing capacity and the skin friction of piles.

The pressure on the tip of a driven pile may be estimated using spherical cavity expansion theory, in which we attempt to model the installation of the pile by the expansion of a cavity within the soil. The analogy is shown in Figure 24. The theory oversimplifies the rather complex process of pile driving, but nevertheless has some merits.

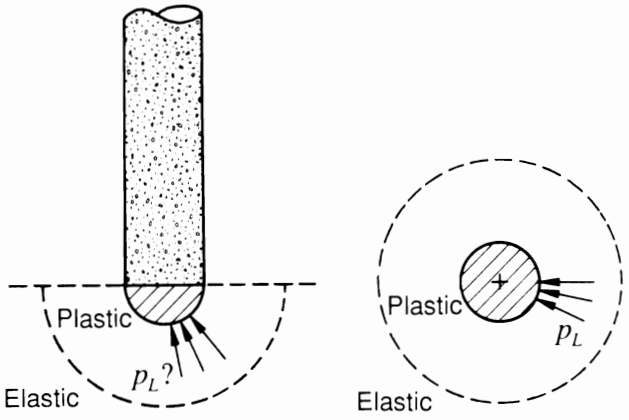

Figure 24, Idealisation of pile end bearing as a spherical cavity expansion

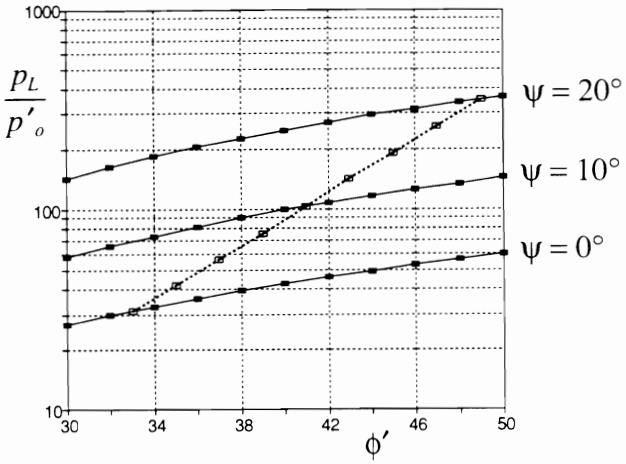

Figure 25, Variation of spherical limit pressure with angle of friction for different dilation angles

The theory of spherical cavity expansion has been modified recently to account for dilation in frictional materials, Yu (1990), Yu and Houlsby (1991). The analysis involves a detailed treatment of the stresses and strains within a zone of soil close to the pile which is deforming plastically, and an outer zone which remains elastic. A detailed explanation would be inappropriate here. The calculated cavity expansion pressures can be used as estimates of the end bearing capacity of piles.

Some examples of the analysis are shown in Figure 25, which shows the variation of the cavity expansion with the angle of friction, for different values of dilation angle. The cavity expansion pressure has been divided by the stress p_o (which must be assumed isotropic) at a large distance from the pile. The three main curves show the pressures calculated for angles of dilation of 0°, 10° and 20°. The other parameters required (constant for all these analyses) are the shear modulus $G = 500p_o$ and Poisson's ratio $\nu = 0.2$. The calculated end bearing capacity increases more than fivefold as the angle of dilation is increased from 0° to 20°, in sharp contrast to the increase of only 13% in the bearing capacity of a surface footing calculated by de Borst and Vermeer for a comparable increase in the dilation angle.

It is clear that dilation plays a much more important role in the highly confined problem of pile bearing capacity than in the relatively unconstrained surface footing problem.

The dilation rate also affects the frictional capacity of piles, but in order to understand its influence in this case, it is first necessary to examine some features of the simple shear test. This is because the deformation of the soil around a pile can

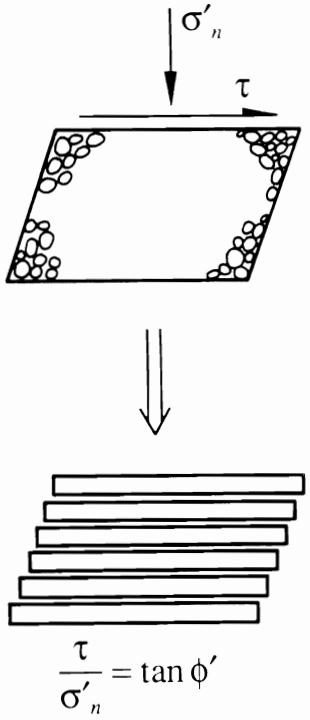

Figure 26, Interpretation of the simple shear test assuming sliding on horizontal planes

be regarded as similar to simple shear. The application the simple shear test to the understanding of pile behaviour was a topic of particular interest to Professor Wroth.

The interpretation of simple shear tests is not straightforward, even when examining a problem apparently as simple as the shear strength. The first assumption that might be made is that the mechanism of failure is one of sliding on horizontal planes, see Figure 26, so that these are planes on which the Mohr-Coulomb condition is satisfied. At failure we therefore have the expected relationship $\tau/\sigma'_n = \tan\phi'$. A closer examination reveals that this assumption is too simplistic in that it has ignored the details of the strain boundary conditions which are imposed on the specimen.

The horizontal plane does not extend, and this condition, together with a knowledge of the fixed dilation rate, fixes the Mohr's circle for strain rate at failure, Figure 27. If we assume that the principal directions of strain rate and of stress coincide, then it is possible to deduce the Mohr's circle for stress. The assumption of the coincidence of the strain rate and stress directions is slightly controversial, and some researchers, notably de Josselin de Jong (1971, 1988) have suggested more complex models in which this assumption is not made. Although such models would produce slightly different calculations, most of the conclusions about pile behaviour made later in this section would still follow.

Knowing the Mohr's circle for stress the ratio of shear to normal stress at failure can be calculated as:

$$\frac{\tau}{\sigma'_n} = \frac{\sin\phi'\cos\psi}{1-\sin\phi'\sin\psi} \qquad \ldots(26)$$

This result is well known, and was independently derived by Davis (1968) and Rowe (1969). It is less well recognised, however, that this equation only refers to the ultimate conditions in a test, and to explore what happens as the test develops it is necessary to use a complete stress-strain model for the soil, accounting for both elastic and plastic deformations. The model used her is a simple elastic-perfectly plastic model in which the elastic strains are given (for the case of plane strain) by:

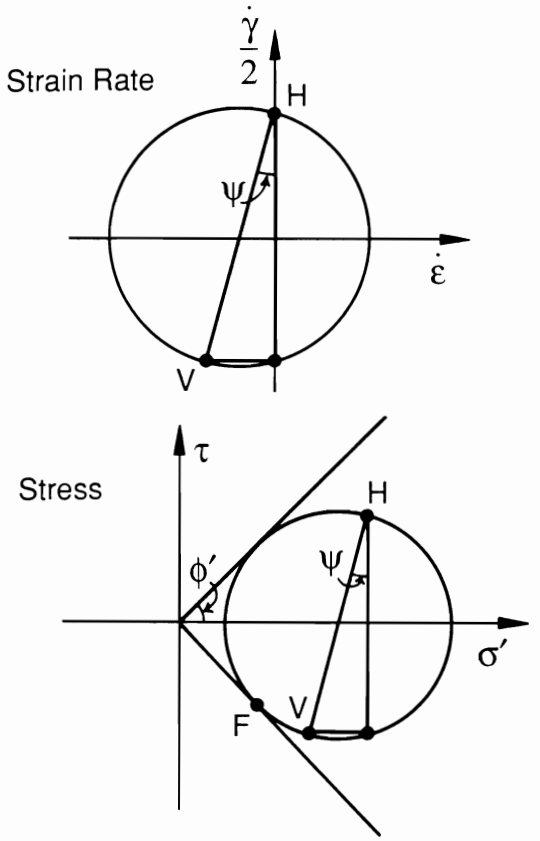

Figure 27, Mohr's circles for strain rate and stress for the simple shear test

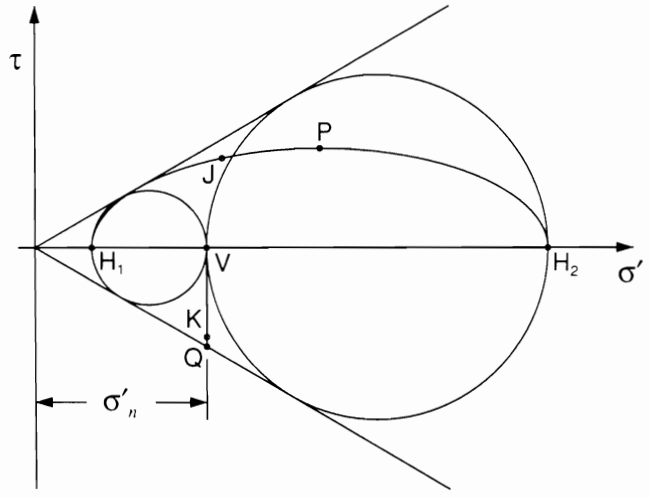

Figure 28, Mohr's circles for simple shear tests with different initial horizontal stresses

$$\begin{bmatrix} \dot{\varepsilon}_{xx} \\ \dot{\varepsilon}_{yy} \\ \dot{\gamma}_{xy} \end{bmatrix} = \begin{bmatrix} (1-\nu^2)/E & (-\nu-\nu^2)/E & 0 \\ (-\nu-\nu^2)/E & (1-\nu^2)/E & 0 \\ 0 & 0 & 1/G \end{bmatrix} \begin{bmatrix} \dot{\sigma}'_{xx} \\ \dot{\sigma}'_{yy} \\ \dot{\tau}_{xy} \end{bmatrix} \quad \ldots(27)$$

the yield surface is given by the Mohr-Coulomb condition:

$$\sqrt{(\sigma'_{xx}-\sigma'_{yy})^2+4\tau_{xy}^2}-(\sigma'_{xx}+\sigma'_{yy})\sin\phi'=0 \quad \ldots(28)$$

The plastic potential is given by an analogous expression in which the angle of friction is replaced by the angle of dilation:

$$\sqrt{(\sigma'_{xx}-\sigma'_{yy})^2+4\tau_{xy}^2}-(\sigma'_{xx}+\sigma'_{yy})\sin\psi+A=0 \quad \ldots(29)$$

where A is a "constant" which depends on the stress point at which yield occurs, and chosen so that the plastic potential passes through that point.

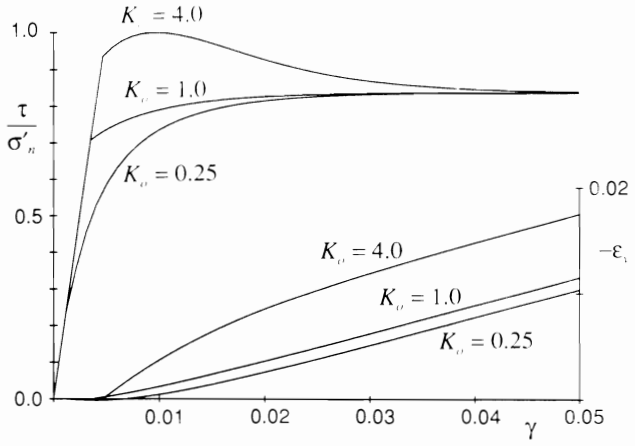

Figure 29, Shear stress - shear strain curves for different initial horizontal stresses

The horizontal stress at the beginning of a simple shear test has an important influence on the results of the test. On the left of Figure 28 is the Mohr's circle for a sample in which the horizontal stress is initially as small as possible. The path during the test of the point representing the stresses on the vertical planes (i.e. the horizontal stress and a shear stress) is from "H_1" to "J", showing how the horizontal stress increases throughout the test. At the same time the point representing the stresses on the horizontal planes (i.e. the vertical stress and a shear stress) moves from "V" to "K". The apparent strength is in this case given the Davis/Rowe expression (Equation 26) and is less than $\tan\phi'$.

If, however, the test begins with a horizontal stress which is as large as possible, then the initial Mohr's circle is as shown on the right of Figure 28. The path representing the horizontal stress is this time from "H_2" to "J", showing that the horizontal stress decreases during the test. The shear stress, however, passes through a peak at point "P", before ending at the same value as before. At the peak the vertical stress is represented by the point "Q". Curiously the *peak* shear strength is given by the original expression $\tau/\sigma'_n = \tan\phi'$, whilst the final value is given by Equation 26. Although effects similar to this have been explored by de Josselin de Jong for a model which does not involve coaxiality of plastic strain rate and stress, it is worth noting that the initial stresses influence simple shear test results even if one adopts a coaxial model.

The stress-strain curves computed using the elastic-perfectly plastic model for three different cases of initial horizontal stress are shown in Figure 29, and demonstrate clearly the peak for the case of a high initial horizontal stress. In order to understand the simple shear test we need therefore to know about the initial stress conditions, and to account properly for them.

The dilation rate of the soil also affects the results of simple shear tests (as can be seen from Equation 26). Figure 30 shows the results for three tests with the same initial stresses and angle of friction, but three different angles of dilation. Not only are the volume changes different, as shown by the lower curves, but the apparent strengths are also different.

Problems such as these are of interest to those who are concerned with the precise interpretation of laboratory tests, but may seem rather remote from practical soil mechanics problems. In fact such calculations are extremely relevant to the difficult task of the prediction of the frictional capacity of bored piles.

When a pile is loaded vertically the behaviour of the soil surrounding the pile could be idealised in the way shown in Figure 31. The actual behaviour will be more complex, but the simple model serves as an illustration.

A relatively thin band of soil close to the pile deforms in simple shear, but in this case it is the vertical strain which is

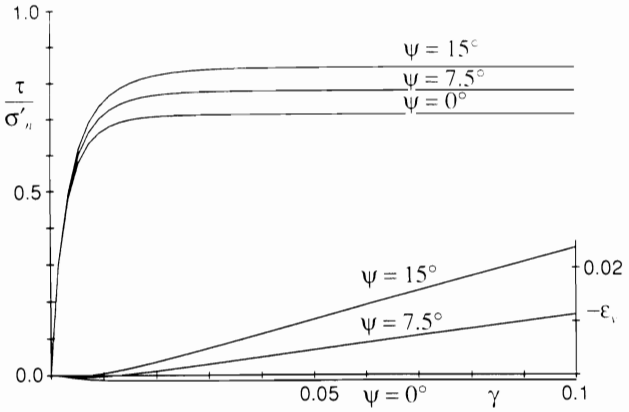

Figure 30, Shear stress - shear strain curves for different dilatancy values

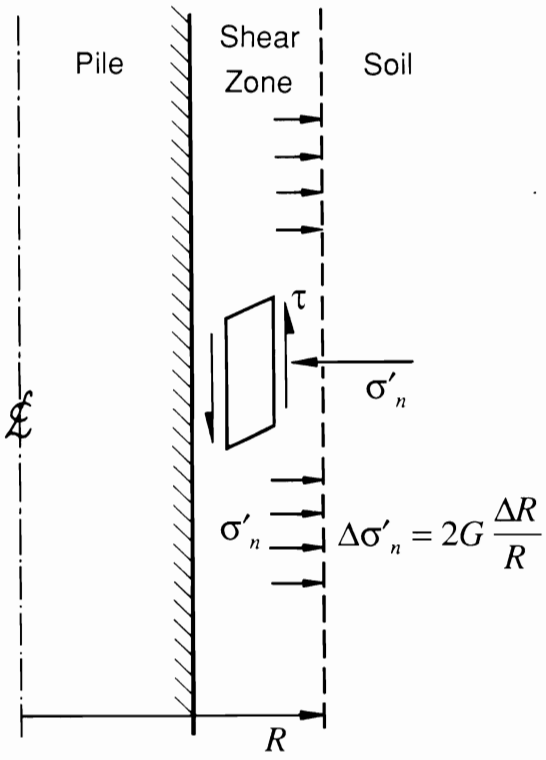

Figure 31, Idealisation of shear zone adjacent to a pile

zero: it is like a conventional simple shear test turned through 90°. As the soil shears it dilates, and so the soil outside this zone is pushed outwards. The result is that the normal stress on the element of soil in simple shear does not remain constant.

The expansion of the surrounding soil can be modelled as analogous to a pressuremeter test, so there is a relationship between the outward movement and the change in normal stress. For simplicity this relationship may be regarded as elastic, and the result is:

$$\Delta\sigma'_n = 2G\frac{\Delta R}{R} \qquad \ldots(30)$$

In practice the distinction between the thin shearing zone (in which the soil is deforming plastically) and the outer zone (in which the soil is assumed to remain elastic) will not be as clear cut as in this simple model. A more complete model could be created using, for instance, one dimensional finite element analysis. The approach adopted here has, however, been used with some success. Johnston, Carter, Novello and Ooi carried out "constant normal stiffness tests" in which the normal stress in a simple shear test was related to the vertical movement, in order to model the behaviour of the soil around piles in carbonate sand.

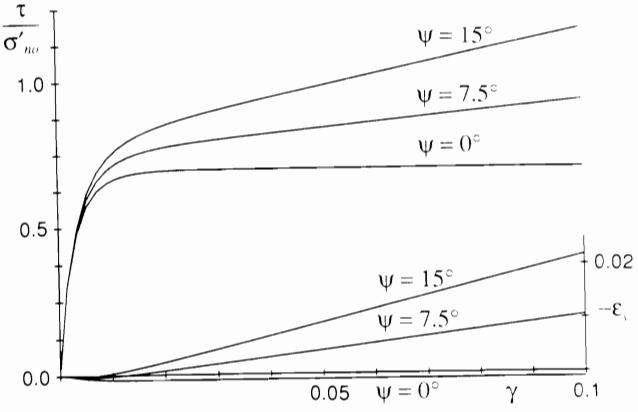

Figure 32, Shear stress - shear strain curves for different dilatancy values and constant normal stiffness

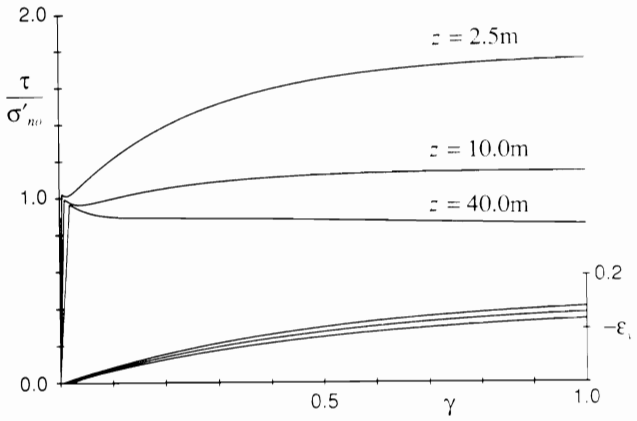

Figure 33, Shear stress - shear strain curves for typical properties for a pile in dense sand

In this model of pile behaviour the dilation becomes very important, because the more the soil dilates, the greater the normal stress becomes. (In the constant normal stiffness tests on carbonate sand the inverse problem occurs: the more the soil crushes the more the normal stress reduces).

Stress-strain curves for the case of constant normal stiffness are shown in Figure 32, for three different dilation angles. The frictional capacity of the pile becomes strongly dependent on dilation. Since a constant angle of dilation has been used in this calculation, both the normal stress and the shear stress increase indefinitely as the sample continues to expand.

More realistic calculations take account of the fact that the angle of dilation reduces as the critical state is approached. The relationship used for the calculations shown in Figure 33 is the one suggested by Wroth (private communication, 1990), as discussed above. The shear stress now approaches a constant value at a large strain. Although the implied strains in the shearing zone are very large, the thickness of this zone is small, so that the associated pile displacements may be small. The calculations are made with three of the sets of values shown in Table 1, which are appropriate for a pile in dense sand. The three curves are for three different points along the length of the pile. At greater depths the stresses in the soil are larger, and so the angle of dilation is smaller. The increase of stress at the pile wall becomes less important at greater depth, and the unit friction on a pile therefore decreases with depth.

The predicted variation of the unit friction on a pile of diameter 0.6m is shown by the solid line on Figure 34, using the values in Table 1. The horizontal axis is the factor "$K \tan\delta$" which is frequently used in pile analysis. It can be seen that the understanding of the importance of dilation can play a key rôle in the understanding of pile behaviour.

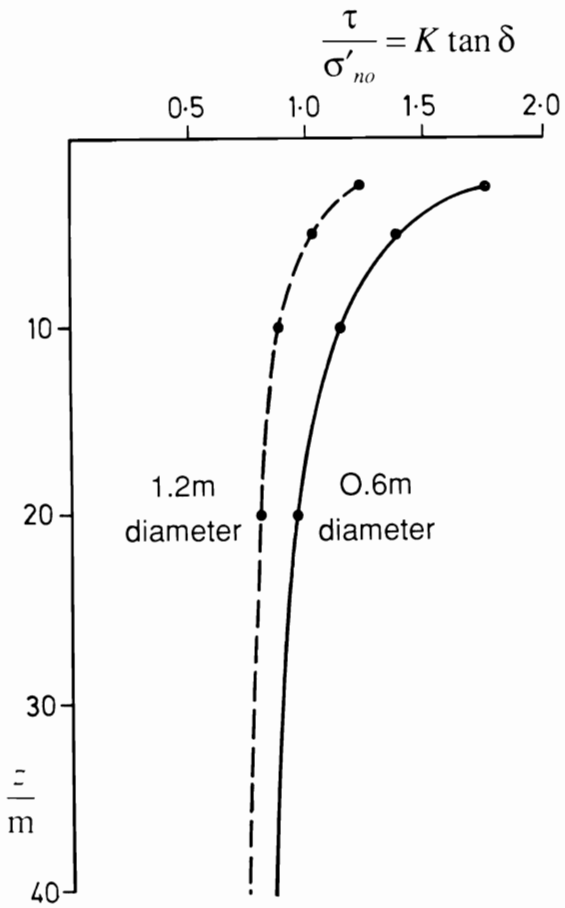

Figure 34, variation of $K \tan\delta$ with depth calculated for piles of different diameters in dense sand

Table 1, Properties used in analysis of frictional capacity of piles

z (m)	σ'_{vo} (kPa)	σ'_{ho} (kPa)	G (MPa)
2.5	25	12.5	2.5
5	50	25	3.5
10	100	50	5
20	200	100	7.1
40	400	200	10
All analyses	$\phi_{cv} = 35°$, $\nu = 0.2$, $\alpha = 1.15$, $\Gamma = 1.88$, $V_o = 1.53$, $\lambda = 0.022$, $R_o = 0.6$m, $h = 0.01$m		

The numerical values shown in Figure 34 depend critically on the estimate of the thickness h of the shearing zone, which may be about 10 to 15 grain diameters thick for a very rough pile. For a relatively smooth steel pile it may be that the failure will occur solely at the pile-soil interface, and the dilatant properties of the soil may be much less important. The results depend in fact on the ratio of the shear zone thickness to the diameter of the pile, and if the zone remains the same thickness then a lower capacity is predicted for larger piles. The broken curve on Figure 34 is computed for a pile of diameter 1.2m, but with all other parameters unchanged. This result has, of course, very significant implications for the use of small scale pile tests, whether in the laboratory or in the field, to predict the behaviour of larger piles. This is a genuine effect of scale which cannot be avoided by, for instance, using a centrifuge to increase the stress level.

The influence of dilatancy in enhancing the horizontal stress on piles has been recognised for some time (see for instance Cernak, Dvorak, Hlavacek, Klein and Petrasek, 1973). Jardine and Christoulas (1991) review evidence of the increase in normal stress on the shaft of a pile due to dilation and discuss some of the factors which influence this increase. The importance of this increase may vary considerably with soil conditions, for instance Frank and Tadjbakhsh (1986) report finite element analyses which give only a modest increase in calculated values of radial stress.

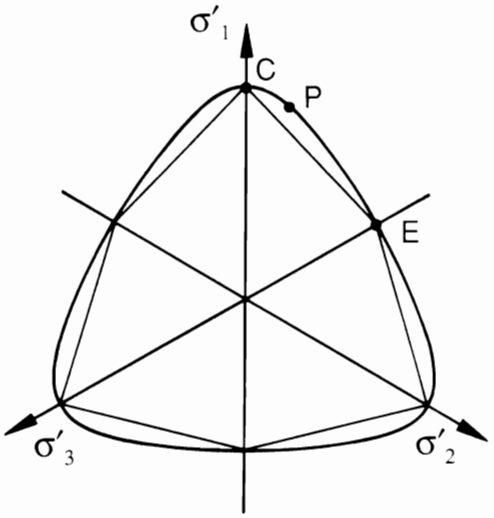

Figure 35, Matsuoka's failure criterion in the octahedral plane

The above examples should show that dilation does not significantly affect the stresses calculated in problems which are relatively unrestrained kinematically, although the deformations will be affected by the dilation angle. In contrast, for problems such as piling, in which strong constraints are placed on the movement of the soil, the fact that the soil is dilating assumes much more importance. The approximate calculations for both the end bearing and frictional capacity of piles demonstrate that dilation can be accounted for using relatively simple soil models.

5 GENERALISATION OF DILATION EXPRESSIONS

It has long been accepted that the angle of friction depends on the mode of shearing as well as other variables such as density and pressure. The angle of friction in plane strain is a few degrees higher than the angle of friction in triaxial compression. This can be understood by examining a plot in the octahedral plane of stress points at failure. This plot is a view looking down the space diagonal in a three dimensional plot of the principal stresses. The Mohr-Coulomb failure criterion for a constant ϕ' value plots as an irregular hexagon. A section at constant p' through the failure surface is shown in Figure 35, in which a test in triaxial compression would plot at "C", a triaxial extension test at "E", and a plane strain test at some point in between.

The observed shape of the failure surface for a sand can be well fitted by an expression suggested by Matsuoka (1976), which gives a smooth curve in this plot:

$$\frac{(\sigma'_1-\sigma'_2)^2}{\sigma'_1\sigma'_2}+\frac{(\sigma'_2-\sigma'_2)^2}{\sigma'_2\sigma'_3}+\frac{(\sigma'_3-\sigma'_1)^2}{\sigma'_3\sigma'_1}=8\tan^2\phi'_{ic} \qquad \ldots(31)$$

Although the Matsuoka expression is a little more complex than the Mohr-Coulomb expression, given an estimate of the intermediate principal stress it is no harder to use. At point "P" in Figure 35 it results in a higher angle of friction in plane strain than in triaxial compression. Lade (1972, 1977) has also suggested an expression for the failure surface which results in a higher angle of friction in plane strain than in triaxial

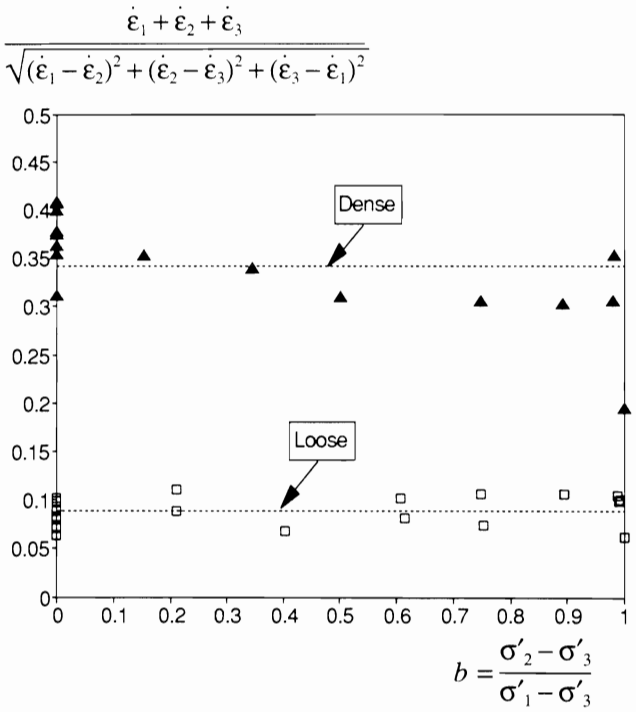

Figure 36, Dilatancy function versus b for Lade's tests on dense and loose sand

compression. His expression differs from Matsuoka's in that it also predicts a slightly higher angle of friction in triaxial extension.

In contrast, very little attention has been paid to changes in the angle of dilation with different modes of shearing, and this variation may be just as important as the variation of the angle of friction. The Author has found that for a number of samples at the same density and sheared in different modes, the peak dilation angles can be modelled by the expression:

$$\frac{(\dot{\varepsilon}_1+\dot{\varepsilon}_2+\dot{\varepsilon}_3)^2}{(\dot{\varepsilon}_1-\dot{\varepsilon}_2)^2+(\dot{\varepsilon}_2-\dot{\varepsilon}_3)^2+(\dot{\varepsilon}_3-\dot{\varepsilon}_1)^2}=\frac{1}{2}\sin^2\psi_{tc} \quad \ldots(32)$$

The expression, which can be seen to be in some ways analogous to Matsuoka's expression for the friction angle, has been tested against true triaxial tests on sand at two different densities by Lade (1972), see Figure 36. The constant required in the new expression is almost independent of the mode of shearing. This expression may therefore provide a way of understanding the relationship between measurements of dilation angles in different types of test.

6 PEAK AND CRITICAL STATE STRENGTH

It is important to introduce a final note of caution. An important consequence of the dilatant properties of soils is that they exhibit peak strengths, followed by a reduction in strength as the critical state is approached. Often we can rely on the large peak strength to be developed, but if there is the possibility of progressive failure then we must be cautious. In Figure 37 the case of a slope failure in which the failure propagates from the toe of the slope is illustrated (more commonly the failure might propagate from the crest). An element of soil at point "A" may have suffered large strain and be past its peak strength by the time the soil at "B" has only just reached peak. At the same time the element at "C" has not yet reached its peak.

In such cases is it not possible for all the soil to achieve its peak strength at the same time, and so the peak strength would be inappropriate for design. The critical state (or constant volume) friction angle ϕ'_{cv}, which can be relied on at large strains, would be more appropriate in this case.

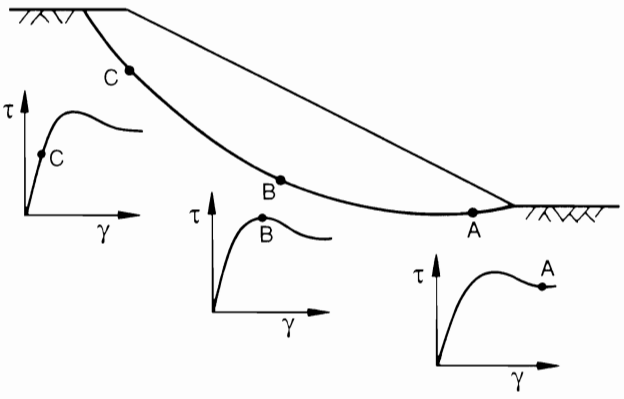

Figure 37, Schematic diagram of stress strain behaviour of points on a slip surface propagating from the toe of a slope

7 CONCLUDING REMARKS

The angle of friction depends on the angle of dilation, which in turn depends on density and pressure. This provides a framework for the understanding of soil behaviour, and explains problems such as the reduction of the peak angle of friction with increasing stress level.

The fact that soil is dilating has an important effect on the solutions to problems where the soil is heavily constrained, as beneath the tip of a pile. It is much less important (except for its effect on the strength) for unconstrained problems such as slope stability.

The dilation of soil can be included in quite simple elastic-plastic models of soil behaviour, and its effects on certain problems explored. More work needs to be done to establish quantitatively how the dilation rate varies with soil conditions, but a suggestion has been made as to how this can be achieved within the framework of Critical State Soil Mechanics.

8 ACKNOWLEDGEMENTS

The Author is grateful to the members of the soil mechanics group at Oxford University for their constructive comments on the content of the spoken version of this paper, and also to Judith Tacaks and John Mooney for their assistance in the preparation of the diagrams. He is also grateful to Dr Roger Frank and Dr Richard Jardine for material for inclusion in the written paper.

9 REFERENCES

Been, K. and Jefferies, M.G. (1985) A State Parameter for Sands, *Géotechnique*, Vol. 35, No.2, 99-112

Bolton, M.D. (1986) The Strength and Dilatancy of Sands, *Géotechnique*, Vol. 36, No. 1, 65-78, Discussion: Vol 37, No. 2, 219-226

Casagrande, A. (1936) Characteristics of Cohesionless Soils Affecting the Stability of Slopes and Earth Fills, *Jour. Boston Soc. Civ. Eng.*, Jan.

Cernak, B, Dvorak, A., Hlavacek, J., Klein, K. and Petrasek, J. (1973) New Approaches to Problems of Bearing Capacity and Settlement of Piles, *Proc. 8th Int. Conf. Soil. Mech. Found. Eng.*, Moscow, 67-74

Davis, E.H. (1968) Theories of Plasticity and the Failure of Soil Masses, in *Soil Mechanics, Selected Topics*, ed. I.K. Lee, Butterworth

de Borst, R. and Vermeer, P.A. (1984) Possibilities and Limitations of Finite Elements for Limit Analysis, *Géotechnique*, Vol. 34, No. 2, 199-210

de Josselin de Jong, G. (1971) The Double Sliding Free Rotating Model for Granular Assemblies, *Géotechnique*, Vol. 21, No. , 155-163

de Josselin de Jong, G. (1988) Elastic-Plastic Version of the Double Sliding Model in Undrained Simple Shear Tests, *Géotechnique*, Vol. 38, No. 4, 533-555

Frank. R. and Tadjbakhsh, S. (1986) Finite Element Study of Pile Axial Behaviour in Elasto-Plastic Dilating Media, *Proc. 3rd Int. Conf. on Numerical Methods in Offshore Piling*, Nantes, May, 201-217

Jardine, R. and Christoulas, S. (1991) Recent Developments in Defining and Measuring Static Piling Parameters, General Report, *Int. Conf. on Deep Foundations*, Paris, March

Lade, P.V. (1972) The Stress-Strain and Strength Characteristics of Cohesionless Soils, Ph.D. Thesis, University of California, Berkeley

Lade, P.V. (1977) Elasto-Plastic Stress-Strain Theory for Cohesionless Soils with Curved Yield surfaces, *Int. Jour. Solids and Structures*, Vol. 13, 1019-1035

Matsuoka, H. (1976) On the Significance of the 'Spatial Mobilised Plane', *Soils and Foundations*, Vol. 16, No. 1, Mar, 91-100

Johnston, I.W., Carter, J.P, Novello, E.A. and Ooi, L.H. (1988) Constant Normal Stiffness Direct Shear Testing of Calcarenite, *Proc. Int. Conf. on Calcareous Sediments*, Perth, Vol. 2, 541-554

Reynolds, O. (1885) On the Dilation of Media Composed of Rigid Particles in Contact, with Experimental Illustrations, *Phil. Mag.*, Vol. 20, 469-481

Rowe, P.W. (1962) The Stress-Dilatancy Relation for Static Equilibrium of an Assembly of Particles in Contact, *Proc. Roy. Soc, Series A*, Vol. 269, 500-527

Rowe (1969) The Relation Between the Shear Strength of Sands in Triaxial Compression, Plane Starin and Direct Shear, *Géotechnique*, Vol. 19, No. 1, 75-86

Schofield A.N. and Wroth C.P. (1968) *Critical State Soil Mechanics*, McGraw Hill, London

Stroud, M.A. (1971) The Behaviour of Sand at Low Stress Levels in the Simple Shear Apparatus, Ph.D. Thesis, University of Cambridge

Taylor, D.W. (1948) *Fundamentals of Soil Mechanics*, Wiley, New York

Wroth, C.P. and Bassett, R.H. (1965) A Stress-Strain Relationship for the Shearing Behaviour of Sand, *Géotechnique*, Vol. 15, No. 1, 32-56

Wroth, C.P. (1958) The Behaviour of Soils and Other Granular Media when Subjected to Shear , Ph.D. Thesis, University of Cambridge

Yu, H.S. (1990) Cavity Expansion Theory and Its Application to the Analysis of Pressuremeters, D.Phil Thesis, University of Oxford

Yu, H.S. and Houlsby, G.T. (1991) Finite Cavity Expansion in Dilatant Soils: Loading Analysis, *Géotechnique*, Vol. 41, No. 2, 173-184

Zienciewicz, O.C., Humpheson, C. and Lewis R.W. (1975) Associated and Non-Associated Visco-Plasticity and Plasticity in Soil Mechanics, *Géotechnique*, Vol. 25, No. 4, 671-689

HOW THE DILATANCY OF SOILS AFFECTS THEIR BEHAVIOUR

by

G.T. Houlsby

The written version of an invited lecture delivered at the Tenth European Conference on Soil Mechanics and Foundation Engineering, Florence, Italy, 28th May 1991

Report Number OUEL 1888/91

Soil Mechanics Report Number 121/91

University of Oxford,
Department of Engineering Science,
Parks Road,
Oxford
OX1 3PJ
U.K

Tel. (0865) 283300
Fax. (0865) 283301

How the Dilatancy of Soils Affects Their Behaviour

De la Manière dont la Dilatance des Sols Influence Leur Comportement

G.T. Houlsby

Department of Engineering Science, Oxford University, U.K.

ABSTRACT: The relationships between the friction angle, dilation angle, density and pressure in a granular material are explored. The link between friction and dilation is well established, but quantitative expressions for the dependance of dilation on density and pressure are less well known. A new relationship based on the concepts of Critical State Soil Mechanics is suggested. The types of problem in which dilation plays an important rôle are then examined, and it is seen that dilatancy increases in significance for heavily constrained problems. The influence of dilation on the capacity of piles is treated in more detail. Additional topics treated include the generalisation of dilation expressions.

RÉSUMÉ: Les relations entre l'angle de frottement, l'angle de dilatance, la densité et la pression dans un milieu granulaire sont étudiées. Le lien entre frottement et dilatance est bien établi, mais les expressions quantitatives de l'influence de la densité et de la pression sur la dilatance sont moins bien connues. Une nouvelle relation basée sur les concepts de la Mécanique des Sols de l'Etat Critique est proposée. Les types de problèmes dans lesquels la dilatance joue un rôle important sont ensuite examinés, et il est montré que la dilatance croît d'une manière significative dans les problèmes à déformation empêchée. L'infuence de la dilatance sur la capacité portante des pieux est traitée d'une manière plus détaillée. Les aspects complémentaires qui sont traités incluent la généralisation des expressions de la dilatance.

1 PREAMBLE

Professor Peter Wroth, of Oxford University, was invited to present a lecture at the Tenth European Conference on Soil Mechanics and Foundation Engineering, and chose as his subject the title of this paper. Sadly, Professor Wroth died in February 1991, and the Author was invited to present a lecture on the same topic in his place. Professor Wroth had not written his lecture, and so this paper is the Author's own views on the subject. The lecture at the Conference, and this written version of it, are presented as the Author's personal tribute to Professor Wroth's wisdom as an engineer, and in gratitude for his many years of encouragement and support.

2 INTRODUCTION

This Paper is divided into two main parts. In the first the relationships between friction, dilation, density and pressure are explored. It is seen that the relationship between the friction angle and dilation angle is well established both theoretically and experimentally. Relationships between the dilation angle and density and pressure are equally important, although less well established quantitatively. Dilation will be seen as occupying a central role in explaining phenomena such as the reduction of angle of friction with increasing stress level.

In the second part of the Paper a series of problems are examined to establish the cases where dilation is important, and it is seen that dilation assumes increasing significance as problems become more kinematically constrained. Particular emphasis is placed in this section on the role of dilation in calculations of the capacity of piles.

Some additional topics are treated at the end of the paper.

3 FRICTION, DILATION, DENSITY AND PRESSURE

The simple frictional model for the failure of a soil, based on Coulomb's pioneering work in 1773, is familiar to all geotechnical engineers, and is conveniently shown on the Mohr's circle diagram, Figure 1. The frictional relationship must of course be expressed in terms of effective, not total, stresses. In the remainder of this Paper the term *stress* shall always mean *effective stress*, and will be indicated by a prime ($'$). The friction angle ϕ' is used to describe the strength of the soil.

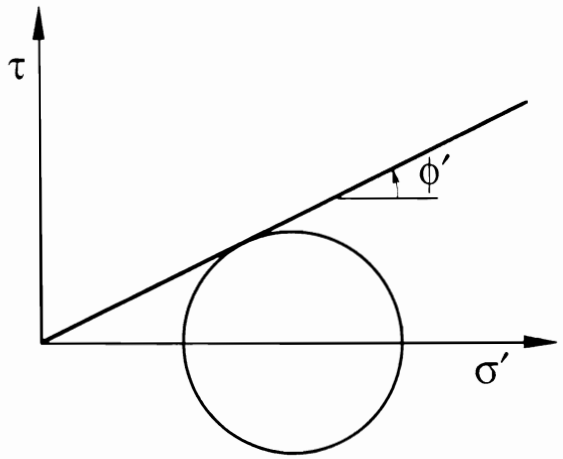

Figure 1, The Mohr-Coulomb failure criterion

Closer examination reveals that the behaviour of soils is more subtle, and shows a number of important features. Firstly, in a test such as the simple shear test on a dense sand, a peak is usually observed in the shear stress - shear strain relationship, followed by a reduction in shear stress at large strain, Figure 2. Similar peaks are observed in other types of shear test. A careful distinction between the peak and large strain angles of friction is therefore necessary, and they are called here ϕ'_p and ϕ'_{cv}.

If the vertical movements, as well as shear displacements, are measured in a simple shear test, then a dense sand usually dilates, that is it expands in volume, as the test proceeds. The dilation usually takes place after a small initial compression, Figure 3. The magnitude of the dilation depends very strongly on the density of the soil, with denser samples expanding more rapidly.

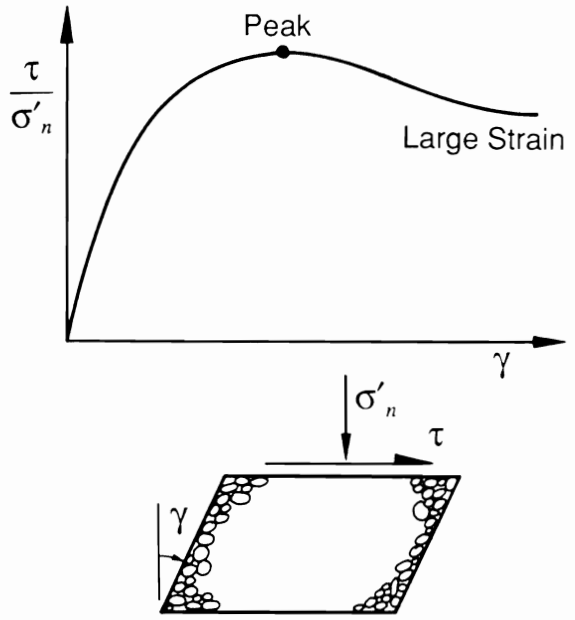

Figure 2, Typical shear stress - shear strain curve in simple shear test

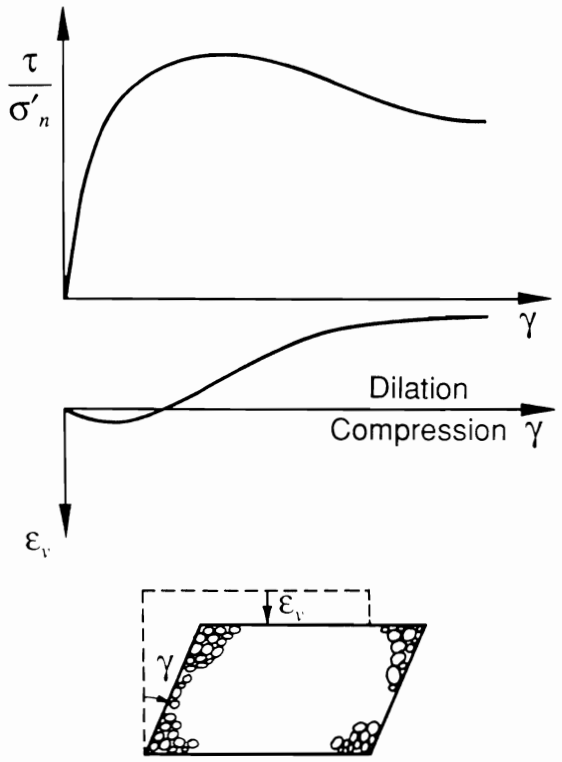

Figure 3, Dilation of dense sand in a simple shear test

If tests are carried out at a number of normal stress levels, it is found that the peak angle of friction reduces with increasing stress level. The result is that the peak strength envelope is curved in the Mohr-Coulomb plot, Figure 4. The peak friction angle approaches the large strain friction angle at very high stress levels.

The features of (a) peak and large strain angles of friction, (b) dilation and the (c) reduction of peak strength with stress level appear at first to be disconnected, and perhaps confusing, phenomena. An important step in the understanding of soil behaviour is the realisation that these features are in fact closely connected, and the understanding of the rôle of dilation is the key to the understanding of how these phenomena are linked. The first step is to appreciate the link between the angles of

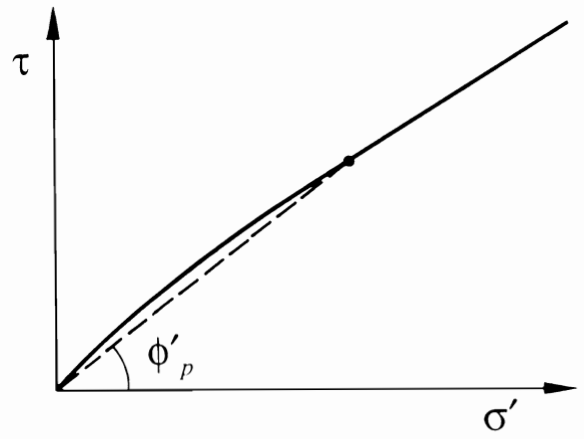

Figure 4, Curved peak strength envelope on Mohr's circle plot

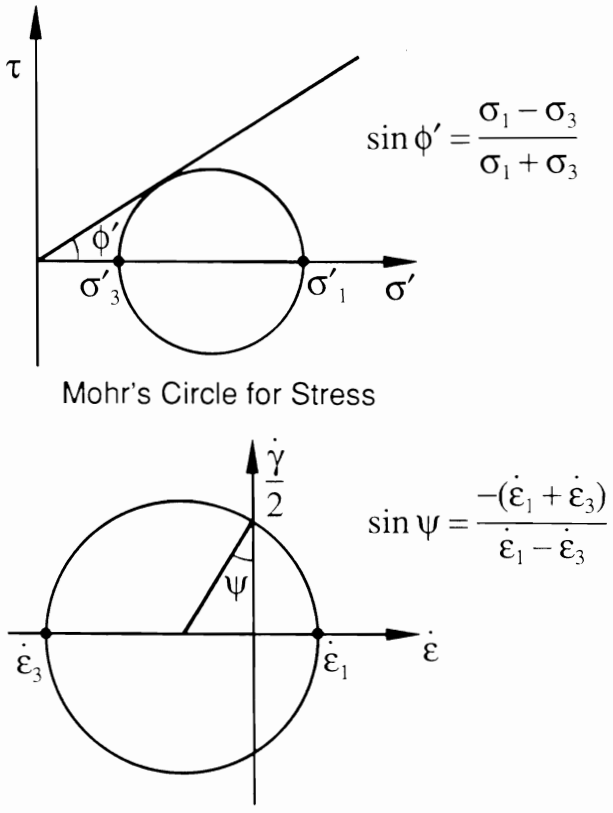

Figure 5, Definitions of the angles of friction and dilation

friction and of dilation; it is then possible to relate the angle of dilation to the density and pressure.

The quantities we must first define are as follows. The angle of friction ϕ' expresses the ratio of a shear stress to a normal stress, and can be defined in terms of principal stresses, Figure 5:

$$\sin\phi' = \frac{\sigma'_1 - \sigma'_3}{\sigma'_1 + \sigma'_3} \qquad \ldots(1)$$

In a similar way the angle of dilation ψ (the symbol ν is also sometimes used for dilation angle) expresses the ratio between a volumetric strain rate and a shear strain rate. For the case of plane strain ($\varepsilon_2 = 0$) it can be defined in terms of the principal strain rates (Figure 5):

$$\sin\psi = \frac{-(\dot{\varepsilon}_1 + \dot{\varepsilon}_3)}{\dot{\varepsilon}_1 - \dot{\varepsilon}_3} \qquad \ldots(2)$$

The minus sign in Equation 2 arises simply from the convention that compressive stresses and strains are taken as positive in soil mechanics, and is introduced so that the angle of dilation is positive when the soil expands.

The superposed dots used in Equation 2 to indicate the strain rates do not imply that the process is in any way dynamic. The term *rate* is being used here in the sense used in plasticity theory, in which the time increment is artificial. The equation could just as well be expressed in terms of strain increments $\delta\varepsilon$ rather than strain rates $\dot{\varepsilon}$.

It is important to note that whilst the definition of the angle of friction remains unchanged for different stress conditions (e.g. triaxial compression, plane strain, triaxial extension), the extension of the definition of the angle of dilation to other than plane strain conditions needs to be treated with more care. The usual definition employed is:

$$\sin\psi = \frac{-(\dot{\varepsilon}_1 + \dot{\varepsilon}_2 + \dot{\varepsilon}_3)}{\dot{\varepsilon}_1 - \dot{\varepsilon}_3} \qquad \ldots(3)$$

which reduces to Equation 2 for plane strain conditions.

A more important distinction is that the angle of dilation should strictly be defined in terms of the *plastic components* of the strain rates, not the total strain rates. If the strain ε is divided into elastic (recoverable) and plastic (irrecoverable) components:

$$\varepsilon = \varepsilon^e + \varepsilon^p \qquad \ldots(4)$$

then Equation 2 should be modified to:

$$\sin\psi = \frac{-(\dot{\varepsilon}_1^p + \dot{\varepsilon}_3^p)}{\dot{\varepsilon}_1^p - \dot{\varepsilon}_3^p} \qquad \ldots(5)$$

In theory this important distinction means that the determination of the angle of dilation from a test becomes much more difficult, since it depends on the estimate which is made for the elastic properties of the soil. In practice the distinction is less important since (for most soils, under most test conditions) the elastic stiffness is sufficiently high that the elastic strains are much smaller than the plastic strains and the difference between Equations 2 and 5 is small. In particular, at the peak in several commonly used shear tests the stresses are not changing, so the elastic strain rates are zero and Equations 2 and 4 coincide. In the remainder of this paper it will be assumed that the elastic strain rates are sufficiently small that Equation 2 can be used with adequate accuracy.

The simplest way to understand the relationship between the angles of friction and dilation is to make use of a physical analogy: the sawtooth model, see Figure 6.

If one frictional block slides over another on a flat plane, with an angle of friction on the plane ϕ'_{cv} (i.e. a coefficient of friction $\mu = \tan\phi'_{cv}$) Then the ratio of the shear to the normal stress is:

$$\frac{\tau}{\sigma'_n} = \tan\phi'_{cv} \qquad \ldots(6)$$

The choice of the subscript "cv" is to indicate that in this case the shearing takes place at constant volume, i.e. no dilation occurs.

If we consider sliding on a rough plane, represented by a sawtooth with teeth at an angle ψ to the horizontal, with the same angle of friction ϕ'_{cv} as above acting on the teeth of the saw, then simple statics can be used to derive the relationship between the observed shear and normal stress when sliding occurs. This ratio could be termed $\tan\phi'$, where ϕ' is the observed angle of friction. It can easily be shown that:

$$\frac{\tau}{\sigma'_n} = \tan\phi' = \tan(\phi'_{cv} + \psi) \qquad \ldots(7)$$

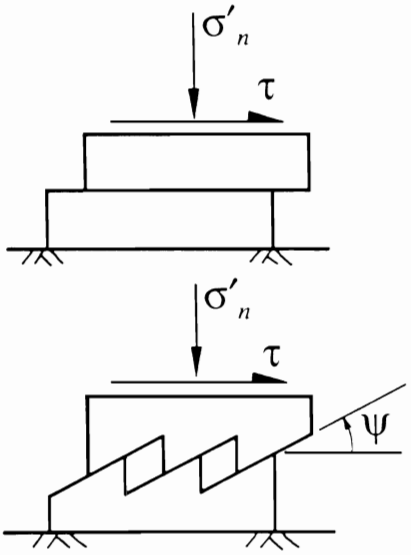

Figure 6, The sawtooth model for dilatancy

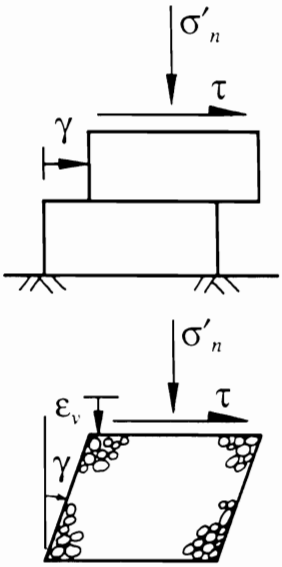

Figure 7, Analogy used in Taylor's energy correction

so that $\phi' = \phi'_{cv} + \psi$, and the observed angle of friction is the sum of the angle of friction at constant volume and the angle of dilation. This type of relationship is called a flow rule.

A variety of other more sophisticated theories have been put forward to explain the relationship between the friction and dilation angles, some of which are discussed below.

One of the first approaches to explain the connection was made by Taylor (1948) who suggested an "energy correction" to account for dilation. In more modern terminology Taylor's expression can be viewed as a hypothesis about the dissipation of work in a frictional soil. All frictional relationships can be viewed in terms of dissipation of energy rather than directly in terms of forces. For a block sliding on a smooth plane (Figure 7), the rate of input work is:

$$\dot{W} = \tau\dot{\gamma} \qquad \ldots(8)$$

and if we adopt the hypothesis that this work is dissipated internally in a way which is proportional to the normal stress σ'_n and the shear strain rate $\dot{\gamma}$, then we have:

$$\dot{W} = (\tan\phi'_{cv})\sigma'_n\dot{\gamma} \qquad \ldots(9)$$

where the constant of proportionality is $\tan\phi'_{cv}$. Combining Equations (8) and (9) yields the familiar result $\tau/\sigma'_n = \tan\phi'_{cv}$.

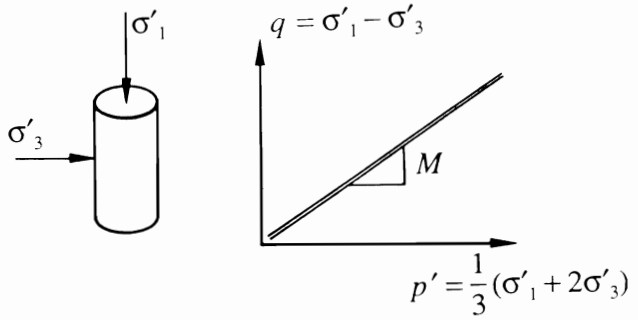

Figure 8, Triaxial parameters used for definition of the Cam-Clay flow rule

The same hypothesis is adopted for a sample of soil in simple shear: that the dissipated work is proportional to the normal stress and the shear strain rate. This time, however, the input work includes a term in σ'_n multiplied by $\dot{\varepsilon}_v$, since dilation may take place and so the normal stress as well as the shear stress does work. The result is therefore:

$$\dot{W} = \sigma'_n \dot{\varepsilon}_v + \tau\dot{\gamma} = (\tan\phi'_{cv})\sigma'_n\dot{\gamma} \qquad \ldots(10)$$

Noting that we could define the apparent angle of friction by $\tan\phi' = \tau/\sigma'_n$, and that the angle of dilation is given by $\tan\psi = -\dot{\varepsilon}_v/\dot{\gamma}$, then Equation 10 can be rearranged to give:

$$\tan\phi' = \tan\phi'_{cv} + \tan\psi \qquad \ldots(11)$$

which differs slightly from the result from the sawtooth model, but again expresses the notion that the angle of friction is equal to the sum of the angle of friction at constant volume and a term which depends on the rate of dilation.

Very similar concepts were used in the development of the Cam-Clay model for soil behaviour (Schofield and Wroth, 1968). The results are usually expressed in terms appropriate for the triaxial test, see Figure 8, and use the stress and strain invariants:

$$p' = \frac{1}{3}(\sigma'_1 + 2\sigma'_3) \qquad \ldots(12)$$

$$q = \sigma'_1 - \sigma_3 \qquad \ldots(13)$$

$$v = \varepsilon_1 + 2\varepsilon_3 \qquad \ldots(14)$$

$$\varepsilon = \frac{2}{3}(\varepsilon_1 - \varepsilon_3) \qquad \ldots(15)$$

The Cam-Clay work hypothesis is expressed as:

$$\dot{W} = p'\dot{v} + q\dot{\varepsilon} = Mp'\dot{\varepsilon} \qquad \ldots(16)$$

which can be seen to be a direct analogy of Taylor's expression (Equation 10). On rearrangement it gives:

$$\frac{q}{p'} = M - \frac{\dot{v}}{\dot{\gamma}} \qquad \ldots(17)$$

which again gives a measure of the angle of friction (q/p', actually equal to $6\sin\phi'/(3-\sin\phi')$), equal to a constant (M) plus a measure of the angle of dilation ($-\dot{v}/\dot{\varepsilon}$, actually equal to $(3\sin\psi)/2$).

The approach taken by Rowe (1962) in the development of his stress-dilatancy theory is conceptually quite different, although it leads to a very similar result. Rowe examined first the properties regular assemblies of spheres, and was able to obtain expressions for both the stress ratio σ'_1/σ'_3 and the strain rate ratio $-\dot{\varepsilon}_3/\dot{\varepsilon}_1$ in terms of the geometry of packing. He then assumed that analogies could be drawn with irregular packings of soil particles. He assumes that sliding takes place on a

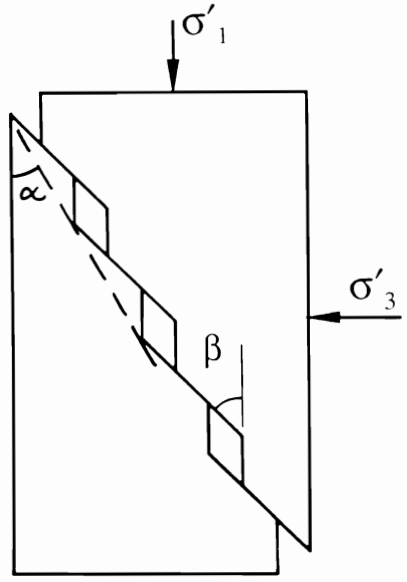

Figure 9, Assumed sliding mechanism for Rowe's stress-dilatancy flow rule

sawtoothed plane, see Figure 9, and these ratios are therefore functions of the angles α and β. The functions are such that α can be eliminated to give:

$$\frac{\sigma'_1}{\sigma'_3} = \frac{\tan(\phi_\mu + \beta)}{\tan\beta}\frac{-\dot{\varepsilon}_3}{\dot{\varepsilon}_1} \qquad \ldots(18)$$

where ϕ_μ is the fundamental angle of friction for grain-to-grain contact. Rowe then adopts a minimum energy *ratio* hypothesis to derive $\beta = \pi/4 - \phi_\mu/2$, but the same result can also be obtained by assuming a minimum stress ratio at a given strain rate ratio. The final result is:

$$\frac{\sigma'_1}{\sigma'_3} = \tan^2\left(\frac{\pi}{4} + \frac{\phi_\mu}{2}\right)\left(\frac{-\dot{\varepsilon}_3}{\dot{\varepsilon}_1}\right) \qquad \ldots(19)$$

which is often written in the short form $R = KD$. The precise rôle of ϕ_μ now becomes unclear, since it now appears as the angle of friction at constant volume. Experimental evidence is, however, that this is not equal to the grain-to-grain friction angle. The discrepancy has been a matter of some debate.

All the methods described above establish theoretical reasons for a connection between the angles of friction and dilation. Experimental evidence for the theories has been presented both by the originators of the theories and by other researchers. Alternatively one could take a mainly empirical approach. Bolton (1986) presented a particularly comprehensive review of the experimental data on friction and dilation angles, and suggested a very simple empirical fit to the data:

$$\phi'_p = \phi'_{cv} + 0.8\psi_{max} \qquad \ldots(20)$$

If the various methods (for the plane strain case) are compared, it can be seen from Figure 10, that the differences are relatively small. Of the theoretical expressions Rowe's falls in the middle of the range, and Bolton's empirical expression matches Rowe's very closely.

It should be noted that these flow rules can be applied in two distinct senses. Firstly they may be used to express the relationship between the *mobilised* angle of friction and the *current* dilation rate as a test progresses. Secondly they may be used to express the relationship between the *peak* friction angle and the *maximum* dilation rate for several tests on the same material. Bolton's empirical relationship is based on the observations of the latter type.

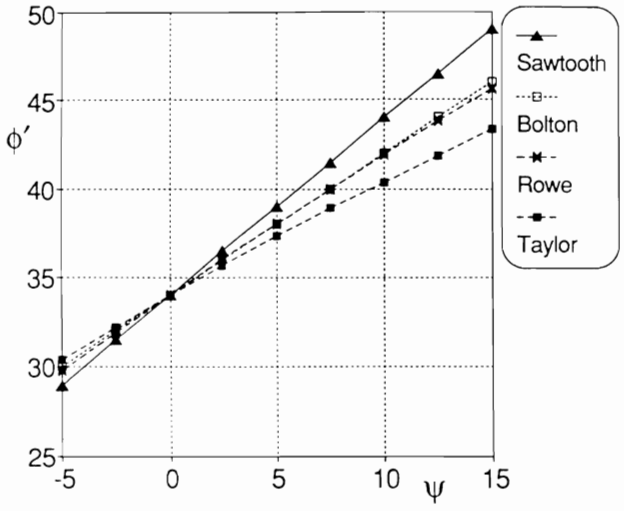

Figure 10, Comparison of flow rules

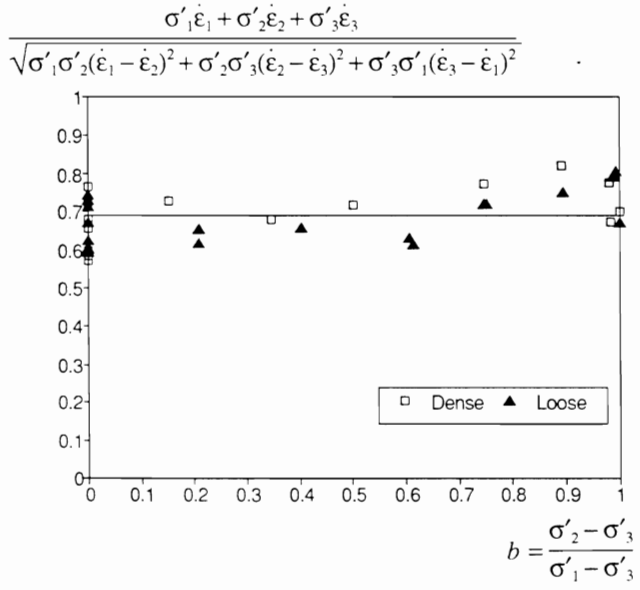

Figure 11, Variation with measured ϕ'_{cvtc} with mode of shearing

One problem in the use of the above flow rules is that the constants employed in them (i.e. ϕ'_{cv}, M or ϕ_μ) need to be changed for different modes of shearing, as the angle of friction at constant volume in plane strain is typically a few degrees higher than that in triaxial compression. Bolton specifically assumes the two angles to be equal, but this is not supported by the experimental evidence. The Author has found that the following work hypothesis provides a flow rule which fits the data from tests with different modes of shearing well:

$$\dot{W} = \sigma'_1\dot{\varepsilon}_1 + \sigma'_2\dot{\varepsilon}_2 + \sigma'_3\dot{\varepsilon}_3 =$$

$$\frac{\sqrt{8}}{3}\tan\phi'_{cvtc}\sqrt{\sigma'_1\sigma'_2(\dot{\varepsilon}_1-\dot{\varepsilon}_2)^2+\sigma'_2\sigma'_3(\dot{\varepsilon}_2-\dot{\varepsilon}_3)^2+\sigma'_3\sigma'_1(\dot{\varepsilon}_3-\dot{\varepsilon}_1)^2} \quad \ldots(21)$$

where ϕ'_{cvtc} is the angle of friction at constant volume in triaxial compression. Figure 11 shows the implied values of ϕ'_{cvtc} evaluated from the peak points from true triaxial tests on sand (Lade, 1972), and shows that this parameter is almost independent of the mode of shearing.

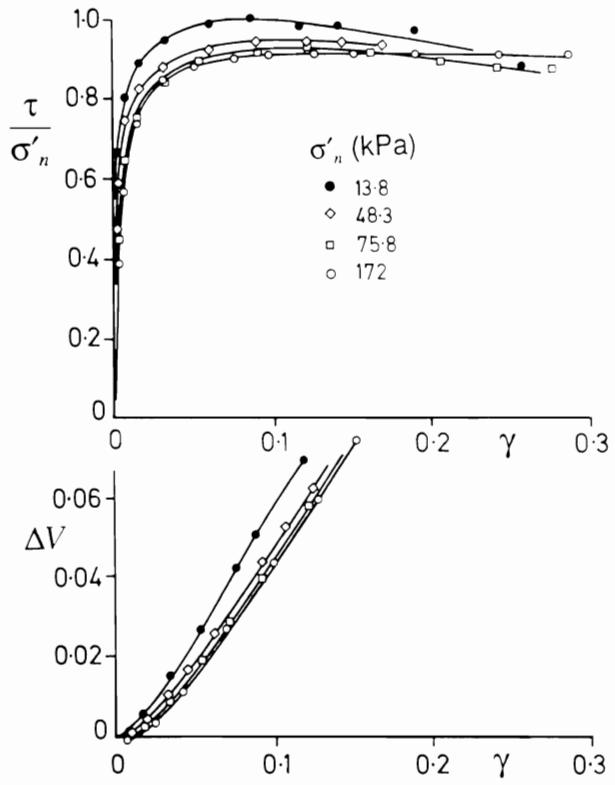

Figure 12, Shear stress - shear strain and volumetric strain - shear strain for simple shear tests on sand (after Stroud, 1971)

It is clear from the above discussion that the relationship between friction and dilation is firmly established both theoretically and experimentally. Although the details of the approaches taken by various authors may differ, the broad conclusions are the same. We turn now to the relationship between dilation and density. It is expected that the denser a sand is the more it will tend to expand, i.e. the higher the dilation angle will be. We find that although this trend is well known, quantitative expressions for the variation of dilation rate with density are much less well established.

One of the best ways of examining the stress-strain behaviour of soils is by simple shear tests, and Stroud (1974) carried out a particularly well controlled set of these tests at Cambridge. The term "simple" refers to the mode of shearing applied to the sample: the apparatus used for the test is in fact rather complex. The upper graph in Figure 12 shows the shear stress-strain curves for his tests on dense sand and the lower curves the change in specific volume with shear strain. Each of these tests started at about the same density, and all showed about the same angle of dilation.

Wroth (1958) had earlier carried out simple shear tests on a variety of materials. These experiments were some of those which formed the basis of what later became known as Critical State Soil Mechanics. Figure 13 shows a set of tests on steel balls, initially packed at different densities. The rate of dilation is higher for denser samples, i.e. those initially at a lower voids ratio. The samples dilate until they reach the same critical voids ratio, irrespective of their initial density, at which they can continue to shear with no further changes of density. The concept of critical voids ratio was not new, being due to Casagrande (1936).

The critical voids ratio is, however, not unique, since it reduces slightly with increasing normal stress. In Figure 14 the end points (i.e. the points where no further changes in voids ratio are occurring) of all of Stroud's tests on sand are plotted in the form of specific volume against mean stress. The points clearly fall on a single line in this plot, with the critical voids ratio reducing with pressure. This leads to the concept of the critical state line. On shearing, all samples will approach this

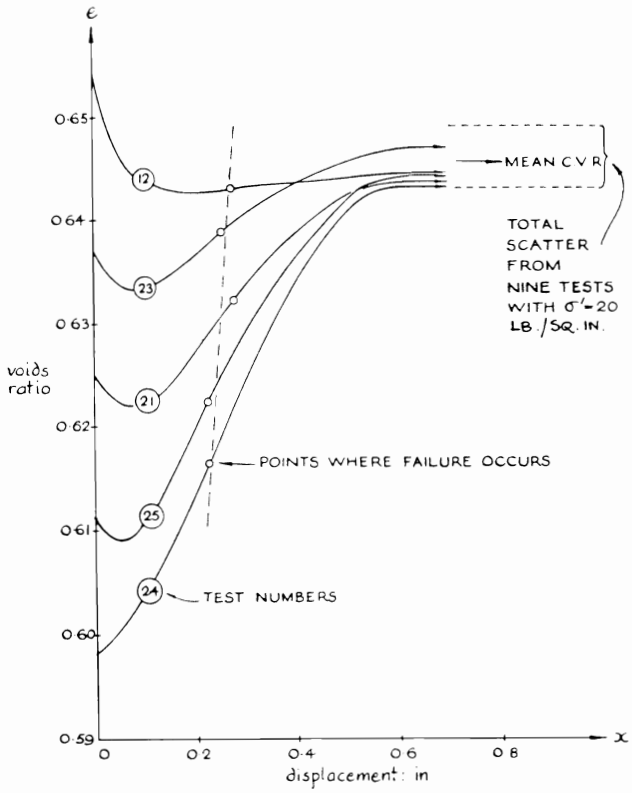

Figure 13, Voids ratio against shear displacement for simple shear tests on steel balls (from Wroth, 1958)

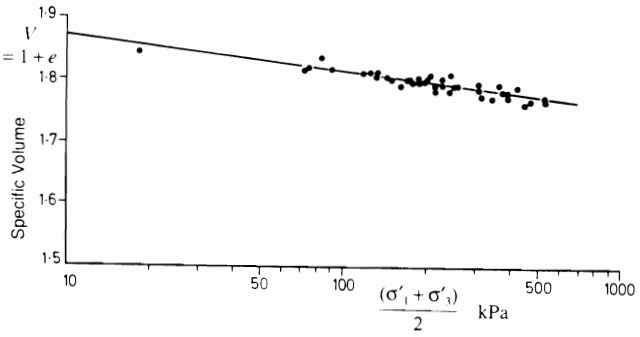

Figure 14, Critical State Line for simple shear tests on sand (after Stroud, 1971)

line, and as they do so will shear with no further change of specific volume, but the actual specific volume they attain will be lower for samples subjected to higher normal pressures. It is observed empirically for clays that the critical state line is parallel to the normal compression line in the consolidation plot.

Stroud's tests covered a range of initial stresses and densities, and the peak angle of friction he observed is shown plotted against pressure in Figure 15. The primary controlling factor for the peak strength is seen to be the density, with denser samples giving a higher strength, but at a given density the angle of friction reduces slightly with increasing stress level. The reduction of the peak strength with stress level is linked to the slope of the critical state line, but in order to establish this connection it is necessary to define some additional quantities.

On the critical state line the rate of dilation is zero, and it seems reasonable that the rate of dilation should simply be a function of the distance of the current stress point from the critical state line. This is expressed by defining the quantities shown in Figure 16. The slope of the critical state line in the V:lnp' plot is λ, and its position is fixed by the value Γ of the

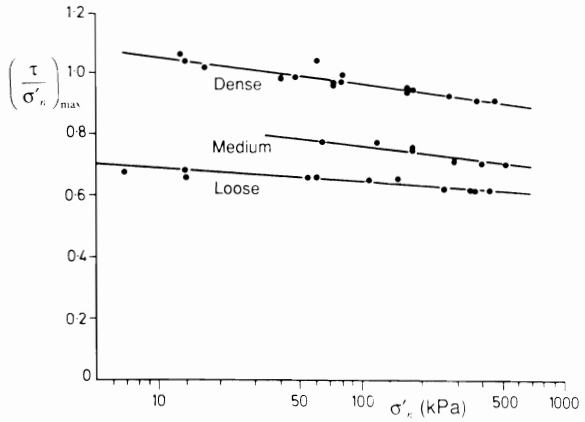

Figure 15, Peak strength against stress level for simple shear tests at different densities (after Stroud, 1971)

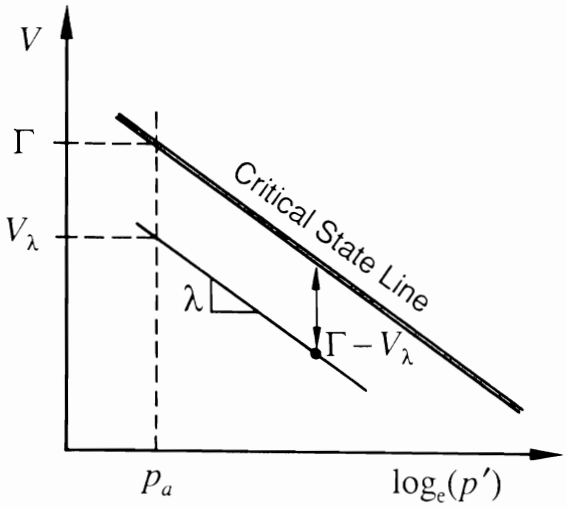

Figure 16, Definitions of Γ and V_λ

specific volume at some reference pressure p_a (conveniently taken as atmospheric pressure). The quantity V_λ, defined as $V + \lambda \ln(p'/p_a)$, is the value of V at p_a on a line drawn through the current point and parallel to the critical state line. Clearly the quantity $(\Gamma - V_\lambda)$ is the distance of the current point below the critical state line. This concept was originally suggested by Wroth and Bassett (1965), and has recently been rediscovered by Been and Jefferies (1985) in their use of the so-called "state parameter".

In Figure 17 the peak strengths from Stroud's tests are plotted against V_λ, and all the tests, from a variety of combinations of pressure and density, plot on a single curve. The peak strength is therefore a unique function of V_λ. In view of the relationships between friction and dilation angles already examined, this also means that the maximum dilation rate is a unique function of V_λ. It is perhaps most helpful to consider the latter relationship as the more fundamental: there are obvious physical reasons why the dilation rate should be higher for denser samples. This result establishes, at least qualitatively, the dependence of the friction and dilation angles on the pressure and density.

Wroth (private communication, 1990) replotted Stroud's data and suggested the simple expression $\sin\psi = \alpha(\Gamma - V_\lambda)$ for the variation of the angle of dilation with distance from the critical state line. The data are shown on Figure 18. The new quantity α is taken as a constant for any given sand, and Wroth found that values of α were typically near unity.

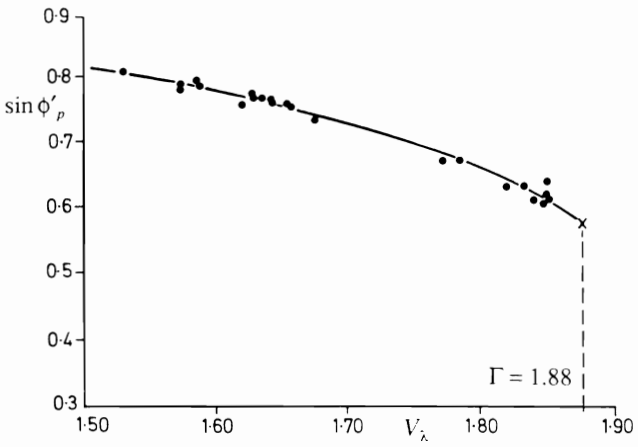

Figure 17, Peak strength plotted against V_λ (after Stroud, 1971)

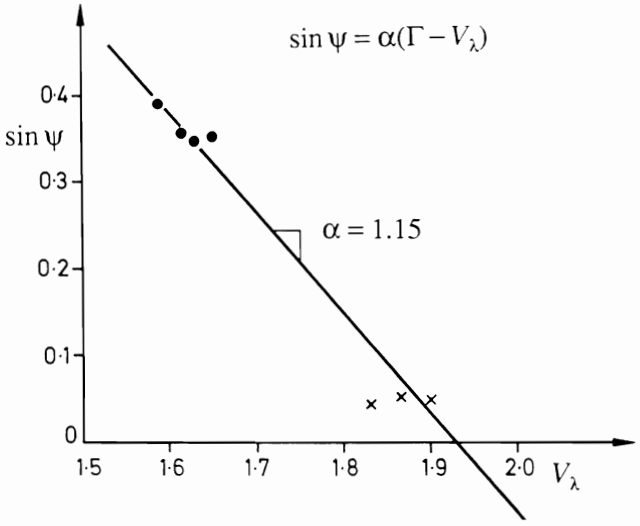

Figure 18, Wroth's interpretation of Stroud's simple shear tests on sand

In practice it is often more convenient to express the behaviour of sand as a function of the relative density I_D rather than the specific volume, and Wroth's expression can be reworked in these terms. The result is the expression:

$$\sin\psi = \alpha(\Gamma - V_{max}) + \alpha(V_{max} - V_{min})I_D - \alpha\lambda\ln\left(\frac{p'}{p_a}\right) \quad \ldots(22)$$

Although this expression looks complex, it is simply of the structure:

$$\sin\psi = A + BI_D - C\ln\left(\frac{p'}{p_a}\right) \quad \ldots(23)$$

where A, B and C are all simple functions of well defined properties of the soil. The angle of dilation (and therefore the angle of friction) increases with density and reduces with pressure. Equation 22 may be compared with the empirical expression suggested by Bolton (1986) for the angle of friction in plane strain (in degrees):

$$\phi'_p = \phi'_{cv} + 5\left(I_D\left[10 - \ln\left(\frac{p'}{1.5p_a}\right)\right] - 1\right) \quad \ldots(24)$$

Together with Equation 20, this can be used to derive an expression for the angle of dilation (in radians):

$$\psi = -0.11 + 0.59I_D - 0.11I_D\ln\left(\frac{p'}{p_a}\right) \quad \ldots(25)$$

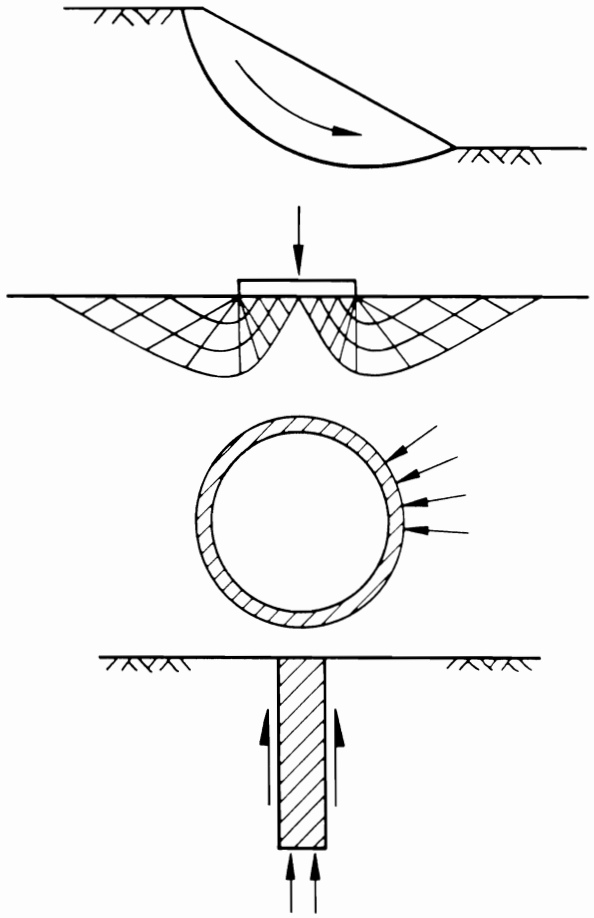

Figure 19, Example problems in increasing order of confinement

Equations 22 and 25 can be seen to be similar in structure, except for the last term. For the range of data available they give almost identical results, and Wroth's expression fits the data as well as Bolton's. Both express the concept that dilation rate (and hence strength) is primarily controlled by density, but also reduces with increasing stress level. The Author prefers Wroth's approach since (a) it directly embodies the concept of the critical state and (b) the constants required can be related to well defined measurable quantities.

If it is possible to estimate the density of a granular material, and the probable value of the working stresses, it is therefore possible to estimate first the dilation rate and then the peak angle of friction.

4 PROBLEMS IN WHICH DILATION IS IMPORTANT

We now examine some cases where the dilation of the soil is important. We should first note that dilation will always be important in that it will control the appropriate angle of friction. The purpose of this discussion is to examine cases where, in addition to this effect, the very fact that the soil is dilating has a further influence on the results.

The importance of dilation will be considered by examining four types of problem in geotechnical engineering, shown schematically in Figure 19. The examples have been ordered in a way that they represent increasing confinement of the soil. In a slope the soil is free to move in a relatively unconfined way. A footing and a flexible tunnel lining impose increasing levels of constraint on the way the soil can deform, and finally the soil in the vicinity of a pile is highly constrained. Intuitively we would expect that the more kinematically constrained the soil is, the more important dilation will be.

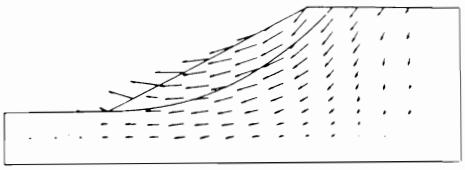

$\psi = 20°$

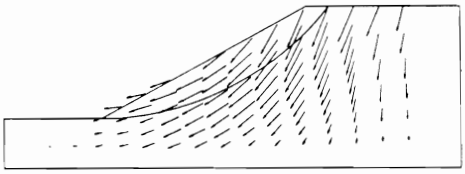

$\psi = 0°$

Figure 20, Deformations of a slope (after Zienciewicz, Humpheson and Lewis, 1975)

The influence of dilation on each of these problems must be examined theoretically, because only in theoretical or numerical analysis can the dilation rate be varied without simultaneously affecting other properties of the soil. Laboratory or field tests would be unable to distinguish the effects of dilation and of friction, since the two, as shown above, are linked for any given material.

The problem of slope stability was examined numerically by Zienciewicz, Humpheson and Lewis (1975). They used the finite element method to carry out two slope stability analyses in which they used the same angle of friction of 20°. In one they assumed the angle of dilation to be equal to the angle of friction, and in the other they assumed zero dilation. The first case in fact gives an impossibly high dilation rate. The analyses resulted in identical factors of safety. However, as would be expected, the patterns of deformation, shown in Figure 20, were rather different. Although this analysis involves a soil with a rather low friction angle, their conclusion that dilation in itself does not affect slope stability seems reasonable.

The problem of the bearing capacity of a footing was also examined by Zienciewicz *et al.* (1975), and they again observed no influence of the dilation rate. It was also examined by de Borst and Vermeer (1984), who carried out finite element analyses of both strip and circular footings on a material with an angle of friction of 40°. They used dilation angles of 40° and 20° (again the first value is impossibly high). The load-deformation curves for circular footings are shown in Figure 21, and the analysis with the higher angle of dilation shows a peak bearing capacity about 13% higher than for the lower dilation angle. At large deformations both analyses approach a similar capacity. It may be that the peak is an artefact of the particular numerical technique involved, but it is more likely that, at least for fairly high friction angles, the rate of dilation does have a small influence on the bearing capacity of a foundation.

As would be expected, the patterns of deformation around the footing, shown much exaggerated in Figure 22, are very different in the two cases. Much larger surface movements are observed for the larger angle of dilation.

The example of the tunnel was also studied by Zienciewicz *et al.* (1975), who made calculations for both the pressures on a tunnel lining, and the ground movements around it for various stages in the construction procedure. The details of the results

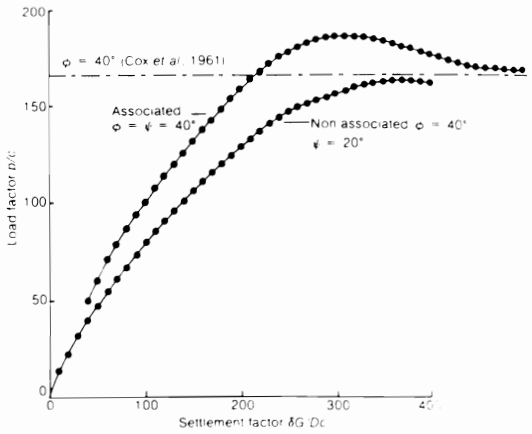

Figure 21, Load - deflection curves for circular footings (after de Borst and Vermeer, 1984)

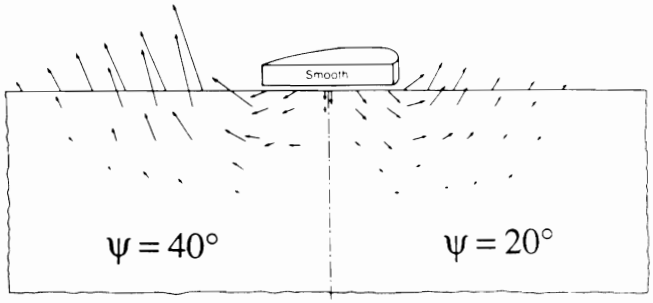

Figure 22, Deformations below a circular footing (after de Borst and Vermeer, 1984)

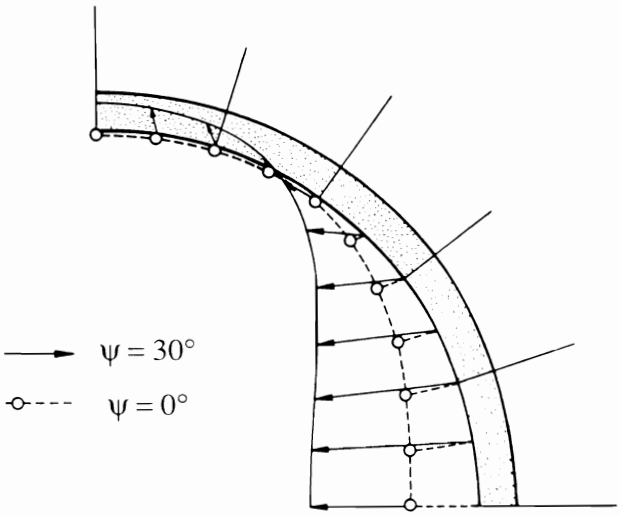

Figure 23, Deformations of a tunnel lining (after Zienciewicz, Humpheson and Lewis, 1975)

must be regarded as specific only to the case they examined, but an example of the influence of the dilation rate on the final deformation of the tunnel lining is shown in Figure 23. Much larger movements are observed for the more dilatant soil.

The conditions around a pile impose much more kinematic constraint on soil movements than for any of the previous problems. We would expect therefore that in a more dilatant soil higher stresses would develop. We shall examine now in rather more detail the influence of dilatancy on both the end bearing capacity and the skin friction of piles.

The pressure on the tip of a driven pile may be estimated using spherical cavity expansion theory, in which we attempt to model the installation of the pile by the expansion of a cavity within the soil. The analogy is shown in Figure 24. The theory oversimplifies the rather complex process of pile driving, but nevertheless has some merits.

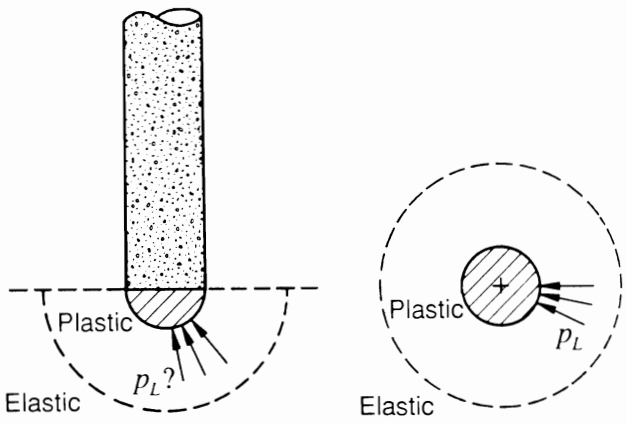

Figure 24, Idealisation of pile end bearing as a spherical cavity expansion

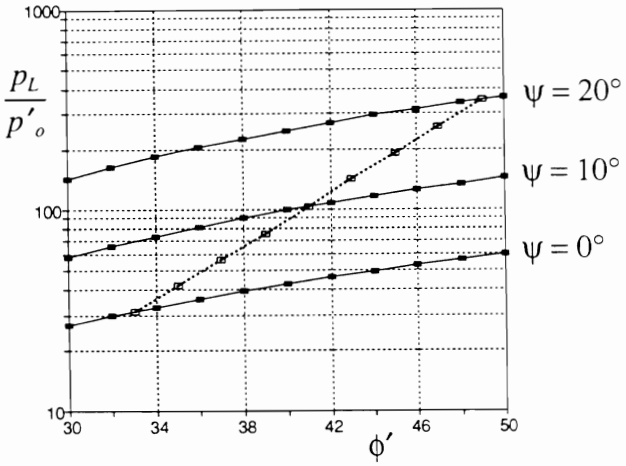

Figure 25, Variation of spherical limit pressure with angle of friction for different dilation angles

The theory of spherical cavity expansion has been modified recently to account for dilation in frictional materials, Yu (1990), Yu and Houlsby (1991). The analysis involves a detailed treatment of the stresses and strains within a zone of soil close to the pile which is deforming plastically, and an outer zone which remains elastic. A detailed explanation would be inappropriate here. The calculated cavity expansion pressures can be used as estimates of the end bearing capacity of piles.

Some examples of the analysis are shown in Figure 25, which shows the variation of the cavity expansion with the angle of friction, for different values of dilation angle. The cavity expansion pressure has been divided by the stress p_o (which must be assumed isotropic) at a large distance from the pile. The three main curves show the pressures calculated for angles of dilation of 0°, 10° and 20°. The other parameters required (constant for all these analyses) are the shear modulus $G = 500p_o$ and Poisson's ratio $\nu = 0.2$. The calculated end bearing capacity increases more than fivefold as the angle of dilation is increased from 0° to 20°, in sharp contrast to the increase of only 13% in the bearing capacity of a surface footing calculated by de Borst and Vermeer for a comparable increase in the dilation angle.

It is clear that dilation plays a much more important role in the highly confined problem of pile bearing capacity than in the relatively unconstrained surface footing problem.

The dilation rate also affects the frictional capacity of piles, but in order to understand its influence in this case, it is first necessary to examine some features of the simple shear test. This is because the deformation of the soil around a pile can

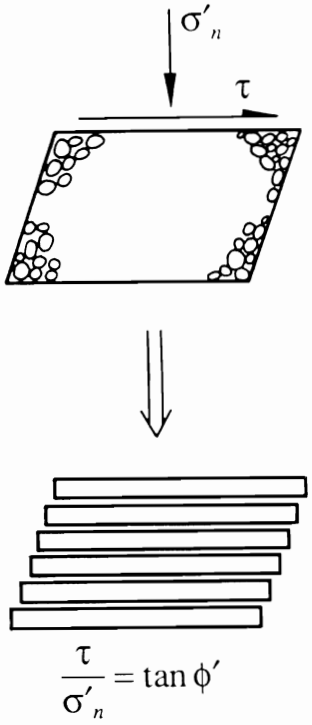

Figure 26, Interpretation of the simple shear test assuming sliding on horizontal planes

be regarded as similar to simple shear. The application the simple shear test to the understanding of pile behaviour was a topic of particular interest to Professor Wroth.

The interpretation of simple shear tests is not straightforward, even when examining a problem apparently as simple as the shear strength. The first assumption that might be made is that the mechanism of failure is one of sliding on horizontal planes, see Figure 26, so that these are planes on which the Mohr-Coulomb condition is satisfied. At failure we therefore have the expected relationship $\tau/\sigma'_n = \tan\phi'$. A closer examination reveals that this assumption is too simplistic in that it has ignored the details of the strain boundary conditions which are imposed on the specimen.

The horizontal plane does not extend, and this condition, together with a knowledge of the fixed dilation rate, fixes the Mohr's circle for strain rate at failure, Figure 27. If we assume that the principal directions of strain rate and of stress coincide, then it is possible to deduce the Mohr's circle for stress. The assumption of the coincidence of the strain rate and stress directions is slightly controversial, and some researchers, notably de Josselin de Jong (1971, 1988) have suggested more complex models in which this assumption is not made. Although such models would produce slightly different calculations, most of the conclusions about pile behaviour made later in this section would still follow.

Knowing the Mohr's circle for stress the ratio of shear to normal stress at failure can be calculated as:

$$\frac{\tau}{\sigma'_n} = \frac{\sin\phi'\cos\psi}{1-\sin\phi'\sin\psi} \qquad \ldots(26)$$

This result is well known, and was independently derived by Davis (1968) and Rowe (1969). It is less well recognised, however, that this equation only refers to the ultimate conditions in a test, and to explore what happens as the test develops it is necessary to use a complete stress-strain model for the soil, accounting for both elastic and plastic deformations. The model used her is a simple elastic-perfectly plastic model in which the elastic strains are given (for the case of plane strain) by:

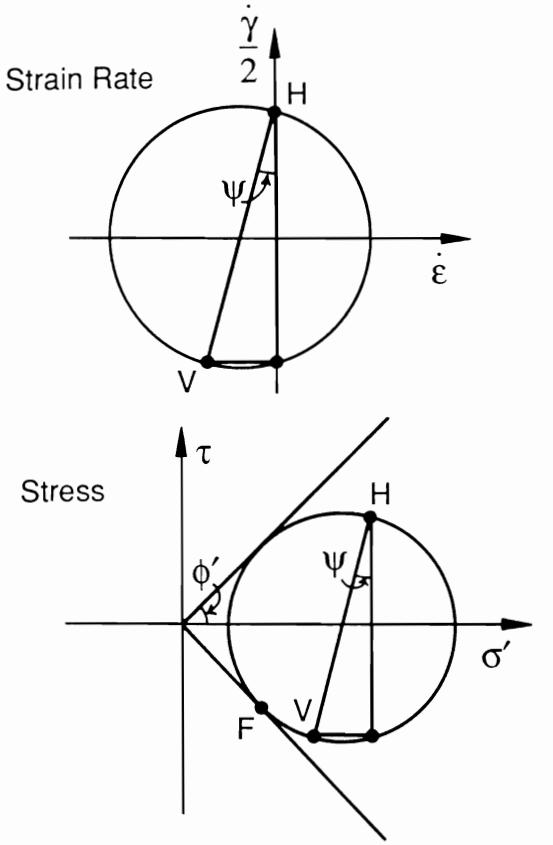

Figure 27, Mohr's circles for strain rate and stress for the simple shear test

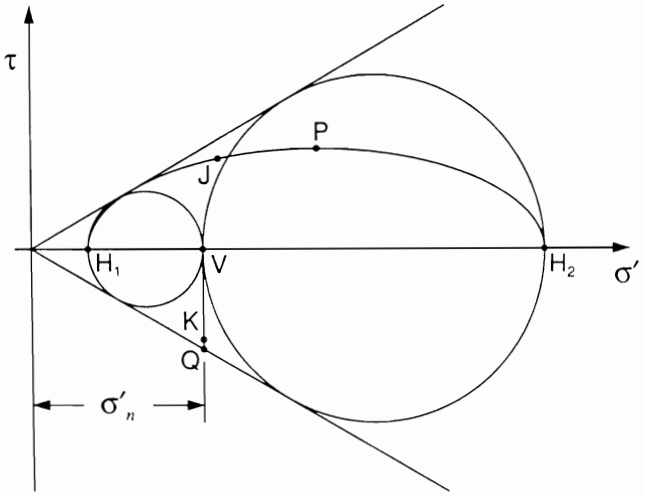

Figure 28, Mohr's circles for simple shear tests with different initial horizontal stresses

$$\begin{bmatrix} \dot{\varepsilon}_{xx} \\ \dot{\varepsilon}_{yy} \\ \dot{\gamma}_{xy} \end{bmatrix} = \begin{bmatrix} (1-\nu^2)/E & (-\nu-\nu^2)/E & 0 \\ (-\nu-\nu^2)/E & (1-\nu^2)/E & 0 \\ 0 & 0 & 1/G \end{bmatrix} \begin{bmatrix} \dot{\sigma}'_{xx} \\ \dot{\sigma}'_{yy} \\ \dot{\tau}_{xy} \end{bmatrix} \quad \ldots(27)$$

the yield surface is given by the Mohr-Coulomb condition:

$$\sqrt{(\sigma'_{xx}-\sigma'_{yy})^2+4\tau_{xy}^2}-(\sigma'_{xx}+\sigma'_{yy})\sin\phi'=0 \quad \ldots(28)$$

The plastic potential is given by an analogous expression in which the angle of friction is replaced by the angle of dilation:

$$\sqrt{(\sigma'_{xx}-\sigma'_{yy})^2+4\tau_{xy}^2}-(\sigma'_{xx}+\sigma'_{yy})\sin\psi+A=0 \quad \ldots(29)$$

where A is a "constant" which depends on the stress point at which yield occurs, and chosen so that the plastic potential passes through that point.

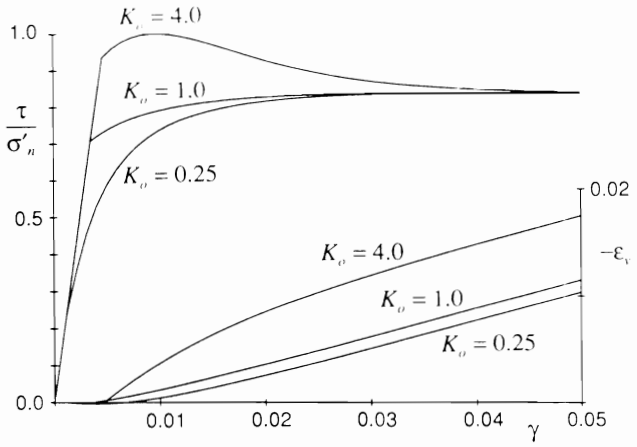

Figure 29, Shear stress - shear strain curves for different initial horizontal stresses

The horizontal stress at the beginning of a simple shear test has an important influence on the results of the test. On the left of Figure 28 is the Mohr's circle for a sample in which the horizontal stress is initially as small as possible. The path during the test of the point representing the stresses on the vertical planes (i.e. the horizontal stress and a shear stress) is from "H_1" to "J", showing how the horizontal stress increases throughout the test. At the same time the point representing the stresses on the horizontal planes (i.e. the vertical stress and a shear stress) moves from "V" to "K". The apparent strength is in this case given the Davis/Rowe expression (Equation 26) and is less than $\tan\phi'$.

If, however, the test begins with a horizontal stress which is as large as possible, then the initial Mohr's circle is as shown on the right of Figure 28. The path representing the horizontal stress is this time from "H_2" to "J", showing that the horizontal stress decreases during the test. The shear stress, however, passes through a peak at point "P", before ending at the same value as before. At the peak the vertical stress is represented by the point "Q". Curiously the *peak* shear strength is given by the original expression $\tau/\sigma'_n = \tan\phi'$, whilst the final value is given by Equation 26. Although effects similar to this have been explored by de Josselin de Jong for a model which does not involve coaxiality of plastic strain rate and stress, it is worth noting that the initial stresses influence simple shear test results even if one adopts a coaxial model.

The stress-strain curves computed using the elastic-perfectly plastic model for three different cases of initial horizontal stress are shown in Figure 29, and demonstrate clearly the peak for the case of a high initial horizontal stress. In order to understand the simple shear test we need therefore to know about the initial stress conditions, and to account properly for them.

The dilation rate of the soil also affects the results of simple shear tests (as can be seen from Equation 26). Figure 30 shows the results for three tests with the same initial stresses and angle of friction, but three different angles of dilation. Not only are the volume changes different, as shown by the lower curves, but the apparent strengths are also different.

Problems such as these are of interest to those who are concerned with the precise interpretation of laboratory tests, but may seem rather remote from practical soil mechanics problems. In fact such calculations are extremely relevant to the difficult task of the prediction of the frictional capacity of bored piles.

When a pile is loaded vertically the behaviour of the soil surrounding the pile could be idealised in the way shown in Figure 31. The actual behaviour will be more complex, but the simple model serves as an illustration.

A relatively thin band of soil close to the pile deforms in simple shear, but in this case it is the vertical strain which is

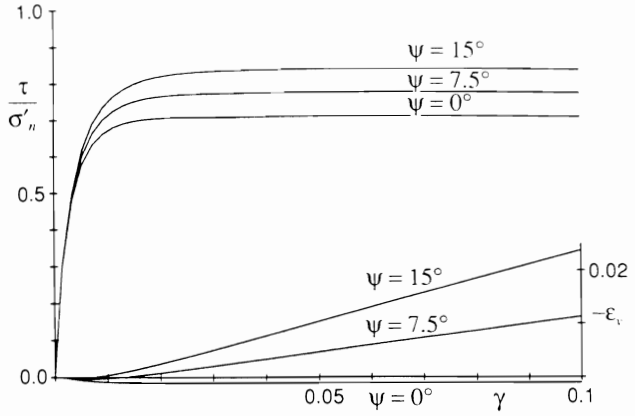

Figure 30, Shear stress - shear strain curves for different dilatancy values

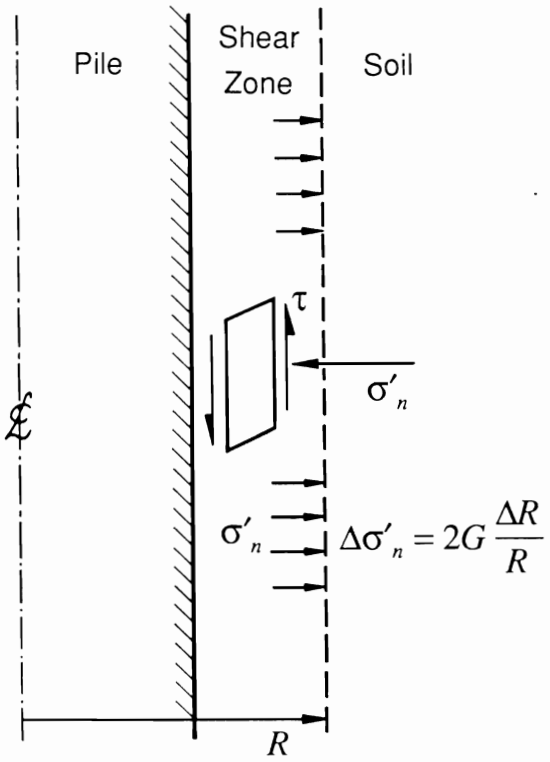

Figure 31, Idealisation of shear zone adjacent to a pile

zero: it is like a conventional simple shear test turned through 90°. As the soil shears it dilates, and so the soil outside this zone is pushed outwards. The result is that the normal stress on the element of soil in simple shear does not remain constant.

The expansion of the surrounding soil can be modelled as analogous to a pressuremeter test, so there is a relationship between the outward movement and the change in normal stress. For simplicity this relationship may be regarded as elastic, and the result is:

$$\Delta\sigma'_n = 2G\frac{\Delta R}{R} \qquad \ldots(30)$$

In practice the distinction between the thin shearing zone (in which the soil is deforming plastically) and the outer zone (in which the soil is assumed to remain elastic) will not be as clear cut as in this simple model. A more complete model could be created using, for instance, one dimensional finite element analysis. The approach adopted here has, however, been used with some success. Johnston, Carter, Novello and Ooi carried out "constant normal stiffness tests" in which the normal stress in a simple shear test was related to the vertical movement, in order to model the behaviour of the soil around piles in carbonate sand.

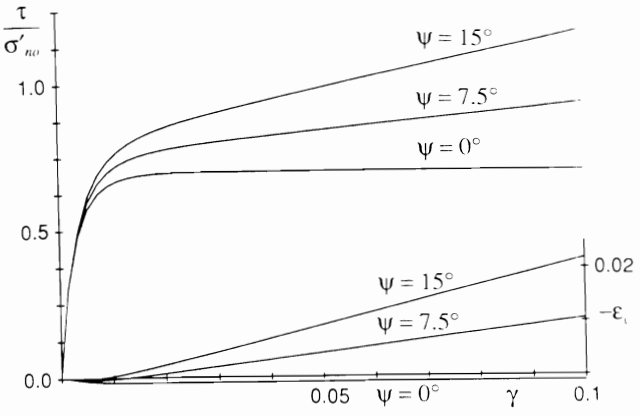

Figure 32, Shear stress - shear strain curves for different dilatancy values and constant normal stiffness

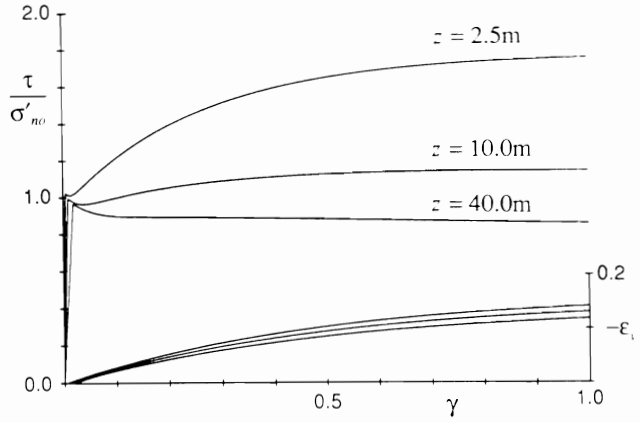

Figure 33, Shear stress - shear strain curves for typical properties for a pile in dense sand

In this model of pile behaviour the dilation becomes very important, because the more the soil dilates, the greater the normal stress becomes. (In the constant normal stiffness tests on carbonate sand the inverse problem occurs: the more the soil crushes the more the normal stress reduces).

Stress-strain curves for the case of constant normal stiffness are shown in Figure 32, for three different dilation angles. The frictional capacity of the pile becomes strongly dependent on dilation. Since a constant angle of dilation has been used in this calculation, both the normal stress and the shear stress increase indefinitely as the sample continues to expand.

More realistic calculations take account of the fact that the angle of dilation reduces as the critical state is approached. The relationship used for the calculations shown in Figure 33 is the one suggested by Wroth (private communication, 1990), as discussed above. The shear stress now approaches a constant value at a large strain. Although the implied strains in the shearing zone are very large, the thickness of this zone is small, so that the associated pile displacements may be small. The calculations are made with three of the sets of values shown in Table 1, which are appropriate for a pile in dense sand. The three curves are for three different points along the length of the pile. At greater depths the stresses in the soil are larger, and so the angle of dilation is smaller. The increase of stress at the pile wall becomes less important at greater depth, and the unit friction on a pile therefore decreases with depth.

The predicted variation of the unit friction on a pile of diameter 0.6m is shown by the solid line on Figure 34, using the values in Table 1. The horizontal axis is the factor "$K \tan\delta$" which is frequently used in pile analysis. It can be seen that the understanding of the importance of dilation can play a key rôle in the understanding of pile behaviour.

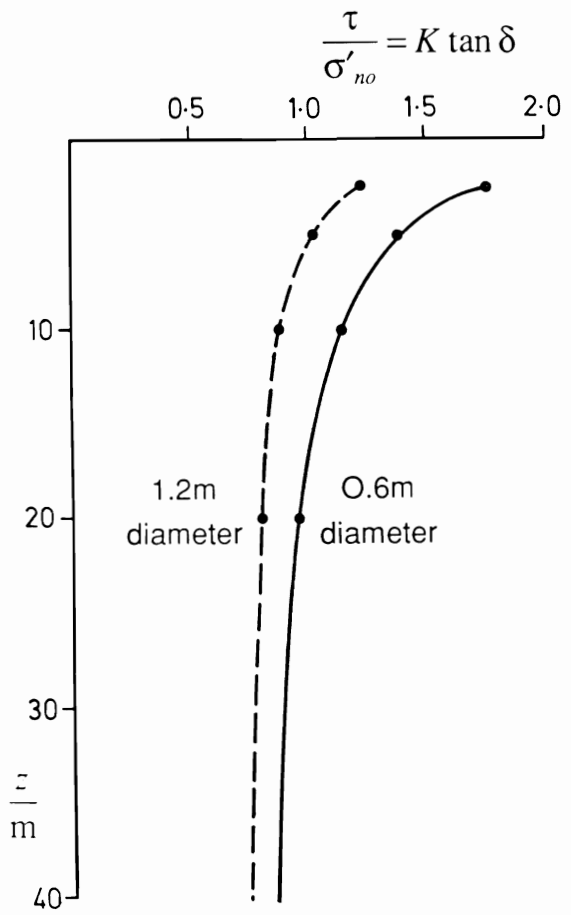

Figure 34, variation of $K \tan\delta$ with depth calculated for piles of different diameters in dense sand

Table 1, Properties used in analysis of frictional capacity of piles

z (m)	σ'_{vo} (kPa)	σ'_{ho} (kPa)	G (MPa)
2.5	25	12.5	2.5
5	50	25	3.5
10	100	50	5
20	200	100	7.1
40	400	200	10
All analyses	$\phi_{cv} = 35°$, $\nu = 0.2$, $\alpha = 1.15$, $\Gamma = 1.88$, $V_o = 1.53$, $\lambda = 0.022$, $R_o = 0.6$m, $h = 0.01$m		

The numerical values shown in Figure 34 depend critically on the estimate of the thickness h of the shearing zone, which may be about 10 to 15 grain diameters thick for a very rough pile. For a relatively smooth steel pile it may be that the failure will occur solely at the pile-soil interface, and the dilatant properties of the soil may be much less important. The results depend in fact on the ratio of the shear zone thickness to the diameter of the pile, and if the zone remains the same thickness then a lower capacity is predicted for larger piles. The broken curve on Figure 34 is computed for a pile of diameter 1.2m, but with all other parameters unchanged. This result has, of course, very significant implications for the use of small scale pile tests, whether in the laboratory or in the field, to predict the behaviour of larger piles. This is a genuine effect of scale which cannot be avoided by, for instance, using a centrifuge to increase the stress level.

The influence of dilatancy in enhancing the horizontal stress on piles has been recognised for some time (see for instance

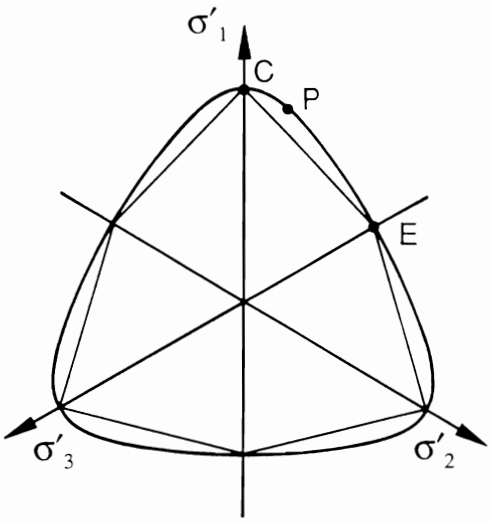

Figure 35, Matsuoka's failure criterion in the octahedral plane

Cernak, Dvorak, Hlavacek, Klein and Petrasek, 1973). Jardine and Christoulas (1991) review evidence of the increase in normal stress on the shaft of a pile due to dilation and discuss some of the factors which influence this increase. The importance of this increase may vary considerably with soil conditions, for instance Frank and Tadjbakhsh (1986) report finite element analyses which give only a modest increase in calculated values of radial stress.

The above examples should show that dilation does not significantly affect the stresses calculated in problems which are relatively unrestrained kinematically, although the deformations will be affected by the dilation angle. In contrast, for problems such as piling, in which strong constraints are placed on the movement of the soil, the fact that the soil is dilating assumes much more importance. The approximate calculations for both the end bearing and frictional capacity of piles demonstrate that dilation can be accounted for using relatively simple soil models.

5 GENERALISATION OF DILATION EXPRESSIONS

It has long been accepted that the angle of friction depends on the mode of shearing as well as other variables such as density and pressure. The angle of friction in plane strain is a few degrees higher than the angle of friction in triaxial compression. This can be understood by examining a plot in the octahedral plane of stress points at failure. This plot is a view looking down the space diagonal in a three dimensional plot of the principal stresses. The Mohr-Coulomb failure criterion for a constant ϕ' value plots as an irregular hexagon. A section at constant p' through the failure surface is shown in Figure 35, in which a test in triaxial compression would plot at "C", a triaxial extension test at "E", and a plane strain test at some point in between.

The observed shape of the failure surface for a sand can be well fitted by an expression suggested by Matsuoka (1976), which gives a smooth curve in this plot:

$$\frac{(\sigma'_1-\sigma'_2)^2}{\sigma'_1\sigma'_2}+\frac{(\sigma'_2-\sigma'_2)^2}{\sigma'_2\sigma'_3}+\frac{(\sigma'_3-\sigma'_1)^2}{\sigma'_3\sigma'_1}=8\tan^2\phi'_{tc} \qquad \ldots(31)$$

Although the Matsuoka expression is a little more complex than the Mohr-Coulomb expression, given an estimate of the intermediate principal stress it is no harder to use. At point "P" in Figure 35 it results in a higher angle of friction in plane strain than in triaxial compression. Lade (1972, 1977) has also suggested an expression for the failure surface which results in a higher angle of friction in plane strain than in triaxial

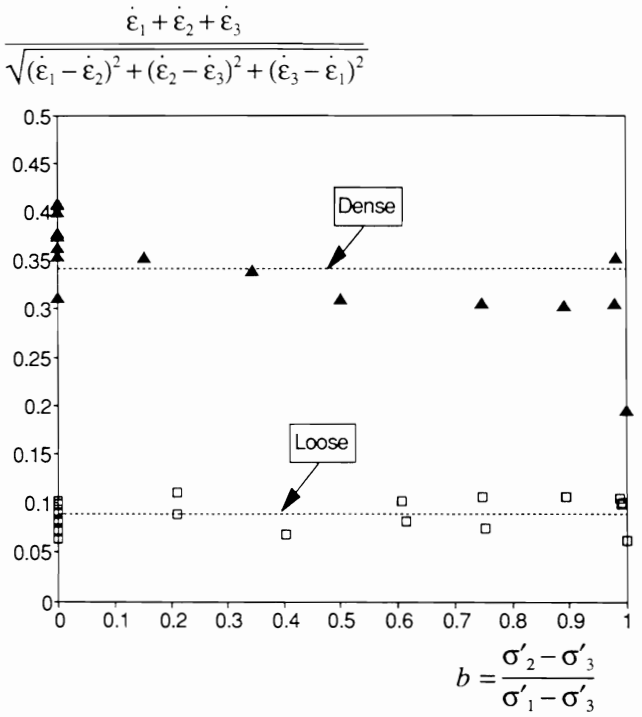

Figure 36, Dilatancy function versus b for Lade's tests on dense and loose sand

compression. His expression differs from Matsuoka's in that it also predicts a slightly higher angle of friction in triaxial extension.

In contrast, very little attention has been paid to changes in the angle of dilation with different modes of shearing, and this variation may be just as important as the variation of the angle of friction. The Author has found that for a number of samples at the same density and sheared in different modes, the peak dilation angles can be modelled by the expression:

$$\frac{(\dot{\varepsilon}_1+\dot{\varepsilon}_2+\dot{\varepsilon}_3)^2}{(\dot{\varepsilon}_1-\dot{\varepsilon}_2)^2+(\dot{\varepsilon}_2-\dot{\varepsilon}_3)^2+(\dot{\varepsilon}_3-\dot{\varepsilon}_1)^2}=\frac{1}{2}\sin^2\psi_{tc} \quad ...(32)$$

The expression, which can be seen to be in some ways analogous to Matsuoka's expression for the friction angle, has been tested against true triaxial tests on sand at two different densities by Lade (1972), see Figure 36. The constant required in the new expression is almost independent of the mode of shearing. This expression may therefore provide a way of understanding the relationship between measurements of dilation angles in different types of test.

6 PEAK AND CRITICAL STATE STRENGTH

It is important to introduce a final note of caution. An important consequence of the dilatant properties of soils is that they exhibit peak strengths, followed by a reduction in strength as the critical state is approached. Often we can rely on the large peak strength to be developed, but if there is the possibility of progressive failure then we must be cautious. In Figure 37 the case of a slope failure in which the failure propagates from the toe of the slope is illustrated (more commonly the failure might propagate from the crest). An element of soil at point "A" may have suffered large strain and be past its peak strength by the time the soil at "B" has only just reached peak. At the same time the element at "C" has not yet reached its peak.

In such cases is it not possible for all the soil to achieve its peak strength at the same time, and so the peak strength would be inappropriate for design. The critical state (or constant volume) friction angle ϕ'_{cv}, which can be relied on at large strains, would be more appropriate in this case.

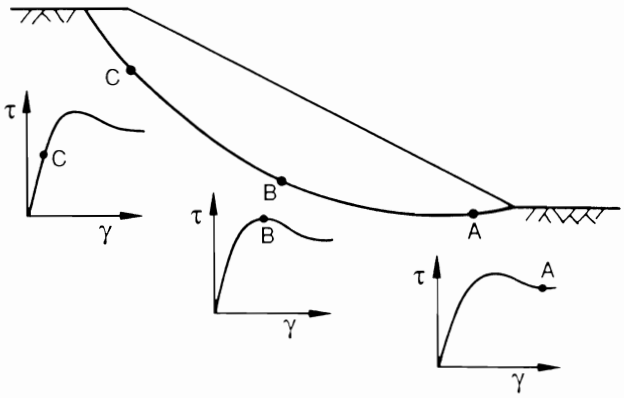

Figure 37, Schematic diagram of stress strain behaviour of points on a slip surface propagating from the toe of a slope

7 CONCLUDING REMARKS

The angle of friction depends on the angle of dilation, which in turn depends on density and pressure. This provides a framework for the understanding of soil behaviour, and explains problems such as the reduction of the peak angle of friction with increasing stress level.

The fact that soil is dilating has an important effect on the solutions to problems where the soil is heavily constrained, as beneath the tip of a pile. It is much less important (except for its effect on the strength) for unconstrained problems such as slope stability.

The dilation of soil can be included in quite simple elastic-plastic models of soil behaviour, and its effects on certain problems explored. More work needs to be done to establish quantitatively how the dilation rate varies with soil conditions, but a suggestion has been made as to how this can be achieved within the framework of Critical State Soil Mechanics.

8 ACKNOWLEDGEMENTS

The Author is grateful to the members of the soil mechanics group at Oxford University for their constructive comments on the content of the spoken version of this paper, and also to Judith Tacaks and John Mooney for their assistance in the preparation of the diagrams. He is also grateful to Dr Roger Frank and Dr Richard Jardine for material for inclusion in the written paper.

9 REFERENCES

Been, K. and Jefferies, M.G. (1985) A State Parameter for Sands, *Géotechnique*, Vol. 35, No.2, 99-112

Bolton, M.D. (1986) The Strength and Dilatancy of Sands, *Géotechnique*, Vol. 36, No. 1, 65-78, Discussion: Vol 37, No. 2, 219-226

Casagrande, A. (1936) Characteristics of Cohesionless Soils Affecting the Stability of Slopes and Earth Fills, *Jour. Boston Soc. Civ. Eng.*, Jan.

Cernak, B, Dvorak, A., Hlavacek, J., Klein, K. and Petrasek, J. (1973) New Approaches to Problems of Bearing Capacity and Settlement of Piles, *Proc. 8th Int. Conf. Soil. Mech. Found. Eng.*, Moscow, 67-74

Davis, E.H. (1968) Theories of Plasticity and the Failure of Soil Masses, in *Soil Mechanics, Selected Topics*, ed. I.K. Lee, Butterworth

de Borst, R. and Vermeer, P.A. (1984) Possibilities and Limitations of Finite Elements for Limit Analysis, *Géotechnique*, Vol. 34, No. 2, 199-210

de Josselin de Jong, G. (1971) The Double Sliding Free Rotating Model for Granular Assemblies, *Géotechnique,* Vol. 21, No. , 155-163

de Josselin de Jong, G. (1988) Elastic-Plastic Version of the Double Sliding Model in Undrained Simple Shear Tests, *Géotechnique,* Vol. 38, No. 4, 533-555

Frank. R. and Tadjbakhsh, S. (1986) Finite Element Study of Pile Axial Behaviour in Elasto-Plastic Dilating Media, *Proc. 3rd Int. Conf. on Numerical Methods in Offshore Piling,* Nantes, May, 201-217

Jardine, R. and Christoulas, S. (1991) Recent Developments in Defining and Measuring Static Piling Parameters, General Report, *Int. Conf. on Deep Foundations,* Paris, March

Lade, P.V. (1972) The Stress-Strain and Strength Characteristics of Cohesionless Soils, Ph.D. Thesis, University of California, Berkeley

Lade, P.V. (1977) Elasto-Plastic Stress-Strain Theory for Cohesionless Soils with Curved Yield surfaces, *Int. Jour. Solids and Structures,* Vol. 13, 1019-1035

Matsuoka, H. (1976) On the Significance of the 'Spatial Mobilised Plane', *Soils and Foundations,* Vol. 16, No. 1, Mar, 91-100

Johnston, I.W., Carter, J.P, Novello, E.A. and Ooi, L.H. (1988) Constant Normal Stiffness Direct Shear Testing of Calcarenite, *Proc. Int. Conf. on Calcareous Sediments,* Perth, Vol. 2, 541-554

Reynolds, O. (1885) On the Dilation of Media Composed of Rigid Particles in Contact, with Experimental Illustrations, *Phil. Mag.,* Vol. 20, 469-481

Rowe, P.W. (1962) The Stress-Dilatancy Relation for Static Equilibrium of an Assembly of Particles in Contact, *Proc. Roy. Soc, Series A,* Vol. 269, 500-527

Rowe (1969) The Relation Between the Shear Strength of Sands in Triaxial Compression, Plane Starin and Direct Shear, *Géotechnique,* Vol. 19, No. 1, 75-86

Schofield A.N. and Wroth C.P. (1968) *Critical State Soil Mechanics,* McGraw Hill, London

Stroud, M.A. (1971) The Behaviour of Sand at Low Stress Levels in the Simple Shear Apparatus, Ph.D. Thesis, University of Cambridge

Taylor, D.W. (1948) *Fundamentals of Soil Mechanics,* Wiley, New York

Wroth, C.P. and Bassett, R.H. (1965) A Stress-Strain Relationship for the Shearing Behaviour of Sand, *Géotechnique,* Vol. 15, No. 1, 32-56

Wroth, C.P. (1958) The Behaviour of Soils and Other Granular Media when Subjected to Shear , Ph.D. Thesis, University of Cambridge

Yu, H.S. (1990) Cavity Expansion Theory and Its Application to the Analysis of Pressuremeters, D.Phil Thesis, University of Oxford

Yu, H.S. and Houlsby, G.T. (1991) Finite Cavity Expansion in Dilatant Soils: Loading Analysis, *Géotechnique,* Vol. 41, No. 2, 173-184

Zienciewicz, O.C., Humpheson, C. and Lewis R.W. (1975) Associated and Non-Associated Visco-Plasticity and Plasticity in Soil Mechanics, *Géotechnique,* Vol. 25, No. 4, 671-689